



Climatology and Interannual Variability of Dynamic Variables in Multiple Reanalyses Evaluated by the SPARC Reanalysis Intercomparison Project (S-RIP)

Craig S. Long¹, Masatomo Fujiwara², Sean Davis^{3,4}, Daniel M. Mitchell⁵, and Corwin J. Wright⁶

5 ¹Climate Prediction Center, National Centers for Environmental Prediction, National Oceanic and Atmospheric Administration, College Park, MD 20740, USA

²Faculty of Environmental Earth Science, Hokkaido University, Sapporo, 060-0810, Japan

³Earth System Research Laboratory, National Oceanic and Atmospheric Administration, Boulder, CO 80305, USA

10 ⁴Cooperative Institute for Research in Environmental Sciences, University of Colorado at Boulder, Boulder, CO 80309, USA

⁵School of Geographical Sciences, University of Bristol, Bristol, UK

⁶Centre for Space, Atmosphere and Ocean Science, University of Bath, Claverton Down, Bath, UK

Correspondence to: Craig S. Long (craig.long@noaa.gov) and Masatomo Fujiwara (fuji@ees.hokudai.ac.jp)

15 **Abstract.** Two of the most basic parameters generated from a reanalysis are temperature and winds. Temperatures in the reanalyses are derived from conventional (surface and balloon), aircraft, and satellite observations. Winds are both observed by conventional systems, cloud tracked, and derived from height fields which in turn are derived from the vertical temperature structure. In this paper we evaluate as part of the SPARC-Reanalysis Intercomparison Project (S-RIP) the temperature and wind structure of all the recent and past reanalyses. This evaluation is mainly between the reanalyses themselves, but comparisons against independent observations such as HIRDLS temperatures are also presented. This evaluation uses monthly mean and 2.5 degree zonal mean data sets and spans the satellite era from 1979 – 2014. There is very good agreement in temperature seasonally and latitudinally between the more recent reanalyses (CFSR, MERRA, ERA-Interim, JRA-55, and MERRA-2) between the surface and 10 hPa. At lower pressures there is increased variance between these reanalyses that changes with season and latitude. This variance also changes during the time span of these reanalyses with greater variance during the TOVS period (1979 – 1998) and less variance afterward in the ATOVS period (1999 – 2014). There is a distinct change in the temperature structure in the middle and upper stratosphere during this transition from TOVS to ATOVS systems. Zonal winds are in greater agreement than temperatures and this agreement extends to lower pressures than the temperatures. Older reanalyses (NCEP/NCAR, NCEP/DOE, ERA-40, JRA-25) have larger temperature and zonal wind disagreement from the more recent reanalyses. All reanalyses to date have issues analysing the Quasi-Biennial Oscillation (QBO) winds. Comparisons with Singapore QBO winds show disagreement in the amplitude of the westerly and easterly anomalies. The disagreement with Singapore winds improves with the transition from TOVS to

20
25
30



ATOVS observations. Temperature bias characteristics determined via comparisons with a Reanalysis Ensemble Mean (MERRA, ERA-Interim, JRA-55) are similarly observed when compared with Aura/HIRDLS and Aura/MLS observations. There is good agreement between NOAA's TLS, SSU1 and SSU2 Climate Data Records and layer mean temperatures from the more recent reanalyses. Caution is advised for using reanalysis temperatures for trend detection.

5

1 Introduction

Reanalyses are used in many ways: as initial conditions for historical model runs, developing climatologies, comparison with experimental models, examination of atmospheric features or conditions over long periods of time, etc. This paper evaluates mainly eight reanalysis data sets: NCEP/NCAR Reanalysis 1 (Kalnay et al., 1996, and Kistler et al., 2001), (referred to hereafter as "R-1"; see Appendix A for abbreviations), ERA-40 (Uppala et al., 2005), JRA-25 (Onagi et al., 2007), NCEP/CFSR (Saha et al., 2010), ERA-Interim (Dee et al., 2011) (referred to hereafter as ERA-I), MERRA (Reinecher et al., 2011), JRA-55 (Kobayoshi et al., 2015), and MERRA-2 (Bosilovich et al., 2016), with some notes on NCEP/DOE Reanalysis 2 (Kanamitsu et al., 2002) (referred to hereafter as "R-2") and 20CR (Compo et al., 2011). See Fujiwara et al. (2017) for more information about these reanalyses. The ERA-15 (Gibson et al., 1997) is not included in this intercomparison due to its short period and subsequent replacement by ERA-40. When a reanalysis product is chosen for use in a study or comparison, the choice is made based upon several factors such as newness of the reanalysis systems, span of time evaluated, horizontal and vertical resolution, top layer, observational data assimilated, etc. In this paper, we present an intercomparison of these ten reanalyses focusing mainly upon their temperature and zonal wind fields, though the mean meridional winds and vertical velocities are also briefly discussed. The five more recent reanalyses (CFSR, MERRA, ERA-I, JRA-55, and MERRA-2) are the primary focus and we concentrate on how these reanalyses intercompare in the upper troposphere and entire stratosphere.

Intercomparisons of middle atmosphere winds and temperatures using reanalyses have been performed since the very first reanalyses were generated in the late 1990's. Pawson and Fiorina (1998a, 1998b, 1999) were the first to evaluate reanalyses winds and temperatures comparing R-1 and ERA-15 analysis of the tropics before and after satellite data were used in the reanalyses, Randel et al. (2004) intercompared wind and temperature climatologies from R-1, ERA-15, ERA-40, along with meteorological centers' analyses. R-1 and the ERA-40 have been used by thousands of researchers for tropospheric studies. Notable middle-atmosphere studies evaluating R-1 and ERA-40 winds and temperatures include the following. Manney et al. (2005) used these two reanalyses along with other analyses to evaluate their ability to capture the unique 2002 Antarctic winter, while Charlton and Polvani (2007) intercompared the two for detecting Northern Hemispheric Sudden Stratospheric Warmings (SSW). Martineau and Son (2010) used temperature and wind fields from R-1, R-2, JRA-25, ERA-I, and MERRA to compare their depiction of stratospheric vortex weakening and intensification events against GPSRO

30



temperature data. Simmons et al. (2014) intercompared the ERA-I, MERRA, JRA-55 stratospheric temperature analyses over the 1979-2012 period showing where and when they agreed and disagreed, and reasons why they did so. They also pointed out the difficulties of the transition from the TOVS to ATOVS observations, most notably in the upper stratosphere-lower mesosphere. Lawrence et al. (2014) used polar processing diagnostics to compare the ERA-I and MERRA. They
5 noted good agreement in the diagnostics after 2002, but cautioned that the choice of one over the other could influence the results of polar processing studies. Miyazaki et al. (2015) intercompared 6 reanalyses (R-1, ERA-40, JRA-25, CFSR, ERA-I, JRA-55) to study the mean meridional circulation in the stratosphere and eddy mixing and their implications upon the strength of the Brewer-Dobson Circulation. Fujiwara et al. (2015) used 9 reanalyses (JRA-55, MERRA, ERA-I, CFSR, JRA-25, ERA-40, R-1, R-2, and 20CR) to examine their stratospheric temperature response to the eruptions of Mount Agung
10 (1963), El Chichón (1982), and Mount Pinatubo (1991). Mitchell et al. (2015) performed a multiple linear regression analysis on the same nine reanalyses to test the robustness of their variability. Martineau et al. (2016) intercompares eight reanalyses (ERA-40, ERA-I, R-1, R-2, CFSR, JRA-25, JRA-55, and MERRA) for dynamical consistency of wintertime stratospheric polar vortex variability. Kawatani et al. (2016) compare the representation of the monthly-mean zonal wind in the equatorial stratosphere, with the focus on the Quasi-Biennial Oscillation (QBO; Baldwin et al., 2001) among nine
15 reanalyses (R-1, R-2, CFSR, ERA-40, ERA-I, JRA-25, JRA-55, MERRA, and MERRA-2).

The report by the SPARC Reference Climatology Group (SPARC, 2002) and the subsequent journal article by Randel et al. (2004) were in response to the need to compare and evaluate then existing middle atmosphere climatologies that were housed and made readily available to the research community at the SPARC Data Center. Both reports provide an intercomparison of eight middle atmosphere climatologies: UK Met Office data assimilation, NOAA Climate Prediction
20 Center objective analysis, UK Met Office objective analysis using TOVS data, Free University of Berlin's Northern Hemisphere subjective analysis, CIRA86 (COSPAR International Reference Atmosphere, 1986), R-1, ERA-15 and ERA-40. This intercomparison was mostly based upon analyses rather than reanalyses, as only the R-1, ERA-15 and ERA-40 reanalyses were available at that time. Notable differences were found between analyses for temperatures near the tropical tropopause and polar lower stratosphere, and zonal winds throughout the Tropics. Comparisons of historical reference
25 atmosphere and rocketsonde temperature observations with the more recent global analyses showed the influence of decadal-scale cooling of the stratosphere. Detailed comparisons of the tropical semiannual oscillation (SAO) and QBO showed large differences in amplitude between analyses; the more recent data assimilation schemes showed better agreement with equatorial radiosonde, rocket, and satellite data (e.g. Baldwin and Gray, 2005).

About 10 years after the SPARC climatology report (SPARC, 2002), SPARC started a new project, the SPARC
30 Reanalysis Intercomparison Project (S-RIP; Fujiwara et al., 2017). The goals of this project are (1) to better understand the differences among current reanalysis products and their underlying causes; (2) to provide guidance to reanalysis data users



by documenting the results of this reanalysis intercomparison; and (3) to create a communication platform between the SPARC community and the reanalysis centres that helps to facilitate future reanalysis improvements. This paper will present the key findings from the S-RIP Chapter 3 team on “Climatology and Interannual Variability of Dynamical Variables.” In this paper we show the results from the eight “full-input” (Fujiwara et al., 2017) reanalyses that are systems that assimilate surface and upper-air conventional and satellite data (i.e., CFSR, MERRA, ERA-I, JRA-55, MERRA-2, JRA-25, ERA-40, R-1), though we will show one figure for 20CR which is one of the “surface-input” reanalyses. We will concentrate only on the satellite era period of 1979 to 2014. Several of the reanalyses do not cover the entire span of the later period (e.g. ERA-40 ends in August 2002, 20CR ends in December 2012 (for its version 2), and JRA-25 ends in January 2014). The R-2 is an updated version of the R-1. Almost all of the changes and enhancements incorporated into the R-2 were surface or boundary layer oriented. The only possible change to the stratosphere would be due to a change to a newer ozone climatology (Fujiwara et al., 2017). As a result, preliminary comparisons of R-1 and R-2 show very minor differences in temperatures and winds above the boundary layer. Therefore, we will not show R-2 comparisons, but one can expect all R-2 qualities to be nearly exactly the same as R-1. All of the reanalyses except for the CFSR used the same forecast model and assimilation scheme throughout their time span. In 2010 the CFSR made an undocumented update to the GSI assimilation scheme, then again in 2011, with the implementation of the version 2 Climate Forecast System (CFSv2, Saha et al., 2014), the resolution, forecast model and assimilation scheme all were upgraded in the CFSR.

The rest of this paper will be organized as follows: Section 2 presents and discusses the reanalyses temperature variability with time. Section 3 presents the methodology used to compare the various reanalyses, the creation of an reanalysis ensemble mean (REM) and the ensemble mean attributes and variability with time. Section 4 presents the differences of the individual reanalyses temperatures and winds from the REM. Section 5 examines the seasonal temperature amplitude of the reanalyses in the polar latitudes. Section 6 discusses the results of comparisons with observations that are not assimilated in the reanalyses by showing specific data analyses. Section 7 provides summaries and main conclusions.

We characterize the stratosphere in altitude ranges using the following generalizations: “upper” for 1 to 5 hPa; “middle” for 7 to 30 hPa; and “lower” for 50 to 100 hPa.

25 **2 Reanalysis Global Mean Temperature Anomaly Variability**

The 1979-2014 period includes the assimilation of satellite observations in addition to the assimilation of conventional (surface, aircraft, and balloon) observations (see Fujiwara et al., 2017 for details). During this period, there are multiple transitions/additions/removals of satellites and instruments observing the atmosphere. The calibration and quality control of the observations from these satellite instruments in many instances have improved over time from the earlier reanalysis systems to the more current reanalysis systems. Also the radiative transfer models used in the forecast models have



improved over time. Reanalysis centers devote major efforts to minimize the transition from one satellite or observing system to the next (e.g., TOVS-to-ATOVS, in 1998; see Fujiwara et al., 2017). However, the forecast models used by the reanalysis centers have their own biases throughout the atmosphere. If and how well the bias correction is performed will also dictate how the reanalysis uses these observations. Additionally, most reanalyses are not run as one stream, but rather it is more efficient timewise and computationally for the reanalysis to be broken up into multiple streams with overlap periods of at least one or more years. These overlap periods are intended to allow the new stream to spin up sufficiently to ensure minimal discontinuity when the older stream ends. Because of these factors, it will be shown that the more recent reanalyses have fewer discontinuities at different times throughout this data record than older reanalyses.

To illustrate how well the various reanalyses were able to transition between satellites and other data sources, Figure 1 presents time series for each reanalysis of the global mean temperature anomalies from their own long term (1979-2014) monthly means. In all of the time series plots, several climatic features are evident: the tropospheric warming during the 1998 and 2010 El Niño events (located on the time axis with an ‘e’), and the stratospheric warming associated with the El Chichón (1982) and Mount Pinatubo (1991) volcanic eruptions (located on the time axis with a ‘v’). However, the older reanalyses (ERA-40 and JRA-25) show several distinct discontinuities in the stratosphere. The ERA-40 shows discontinuities during several changes of the NOAA polar satellites with the SSU instrument in the early 1980’s. The JRA-25 shows smaller discontinuities in the 1980’s, but has an abrupt change in 1998 coincident with the transition from TOVS (SSU, MSU) to the ATOVS (AMSU) observing systems. Of the five more recent reanalyses, the CFSR shows multiple discontinuities in the upper and middle stratosphere. This is because the CFSR is made up of six streams (end years: 1986, 1989, 1994, 1999, 2005, 2009) and also because it corrects the biases in the SSU channel 3 observations with a forecast model that has a noted warm bias in the upper stratosphere. The ERA-I shows two distinct discontinuities: in 1985 from the transition from NOAA-7 SSU to NOAA-9 SSU and in August 1998 from the immediate transition from TOVS to ATOVS observing systems. MERRA merged the SSU and AMSU observations over a period of time. They immediately stopped using the SSU Channel 3 in October 1998 but continued to assimilate channels 1 and 2 through 2005. JRA-55 also merged the SSU and AMSU observations, but for a shorter overlap period of one year. MERRA-2 immediately transitions from SSU and MSU to the AMSU in 1998 and then shows another transition when it begins using Aura/MLS observations in August 2004. R-1, R-2, and the 20CR reanalyses only extend up to 10 hPa, so the upper stratosphere is not analyzed. R-1 and R-2 use NESDIS derived temperature retrievals, which minimized satellite transitions. The 20CR is shown as an example that assimilated only surface based observations. Therefore, it shows no discontinuities, but its forecast model included the volcanic aerosols and the historical changes in carbon dioxide to produce inter-annual variations in the stratosphere (see Fujiwara et al., 2017 for more details).



5 The timing and degree of these discontinuities will play a role in how well the various reanalyses compare with each other over time. Difficulties associated with assimilating the SSU observations due to their CO₂ pressure modulated cells slowly leaking and the changing of atmospheric CO₂ impaired the earlier reanalyses (ERA-40, JRA-25). The more recent reanalyses should agree more closely with each other after 1998 because there are fewer issues assimilating the ATOVS observations.

Because of these discontinuities and transitions discussed above, reanalyses should be viewed very skeptically for use in trend analysis and trend detection, especially in the middle and upper stratosphere.

3 Reanalysis Ensemble Mean (REM)

3.1. Methodology

10 No one reanalysis is the *de facto* standard for all variables and processes. Consequently a reanalysis ensemble mean (REM) of three of the more recent reanalyses (MERRA, ERA-I, and JRA-55) will be used as the reference from which differences and anomalies will be determined. The CFSR is excluded from the REM primarily because of the stream-change impacts upon the temperature structure in the middle and upper stratosphere. MERRA-2 is not included in the REM because it had just become available at the time of the preparation of this paper and does not include 1979. The data sets used to
15 perform the intercomparisons are monthly mean zonal means at 2.5° resolution. Standard post-processed pressure levels are used (1000, 850, 700, 500, 400, 300, 250, 200, 150, 100, 70, 50, 30, 20, 10, 7, 5, 3, 2, 1 hPa). The focus time period of this intercomparison is 1979 through 2014. The current WMO 30-year climatology period (1981-2010) will be the base period of the climatology used. It should be noted that most reanalyses, with the exception of MERRA and MERRA-2, provide
20 data below the surface for some regions (e.g. at 1000 hPa over the Antarctica and Tibetan Plateau). These data are calculated via vertical extrapolation. When the REM is created, re-gridded zonal means are first calculated for each reanalysis, and then the three data sets are averaged where valid data exist. Since most of the latitude zones poleward of 60° S are part of the Antarctic land mass with surface elevations reaching 3 kilometers pressures higher than 700 hPa have invalid data and hence are not analyzed.

3.2 Climatology of the REM

25 3.2.1 Temperature

The seasonal variation of the REM temperature monthly means and their interannual variability in three different zonal regions (60°-90° N, 10° S-10° N, and 90°-60° S) are shown in Figure 2. Of note is that at polar latitudes the lowest temperatures occur in the upper stratosphere in November (for Northern Hemisphere, NH) and May (for Southern



Hemisphere, SH) and descend with time such that the lowest temperatures in the lower stratosphere do not occur until January in the NH and September in the SH. Thus, when lower stratospheric temperatures are reaching a minimum, upper stratospheric temperatures are already increasing. The lowest temperatures occur at about 30 hPa in both polar regions. However, the lowest SH polar temperatures are more than 15 K colder than the lowest NH polar temperature. The interannual variability graphs show that the greatest variability in the NH temperatures is in the upper stratosphere in February when wave activity is most pronounced. In the SH the greatest variability occurs in October and November, associated with the winter to spring transition from low to high temperatures, when wave activity becomes significant in that hemisphere. This variability is associated with how quickly that transition occurs. In some years the circulation over Antarctica is very zonal and stable, which prolongs the period of low temperatures in the polar latitudes. In other years there may be more wave activity transporting heat from the extra-tropics into the polar latitudes, thus shortening the period of low temperatures in the polar latitudes. In the tropics, the variability is much smaller than in the polar regions, but is associated with the SAO and with the QBO in the middle and upper stratosphere.

3.2.2 Zonal Wind

The seasonal variation of the REM zonal wind monthly means and their interannual variability in three different zonal regions (40° - 80° N, 10° S- 10° N, and 80° - 40° S) are shown in Figure 3. In the NH polar jet region (40° - 80° N) the maximum winds occur in the upper stratosphere in November and December, and the greatest variability occurs from December through March. In the SH polar jet region (80° - 40° S) wintertime westerlies are about 30 m/s stronger than the winter time NH westerlies. These stronger westerlies are due to the much weaker disruption of the polar vortex by the vertically-propagating planetary-scale waves. Similar with the temperature variability, the variability of the SH polar night jet between May through August is not as great as in the NH polar jet. The SH zonal wind variability does increase during the final warming and transition from westerlies to easterlies as wave activity increases from August through November.

In the tropical upper stratosphere, there is a strong semi-annual oscillation (SAO; Ray et al., 1998) with maximum westerlies of up to 20 m/s at equinox and intervening easterlies during the solstice periods. There is a marked asymmetry in amplitude of the easterly SAO phase, with amplitudes of -40 to -50 m/s easterlies in December-to-February but only -20 to -30 m/s in July-September. The easterly SAO phase is believed to result from advection of easterlies from the summer hemisphere by the Brewer-Dobson circulation, and this asymmetry is consistent with the much stronger circulation in December-to-February associated with greater wave activity in the NH winter. In the equatorial mid-stratosphere where the QBO dominates, the climatological winds in the tropical middle stratosphere have mean easterlies of -5 to -10 m/s. Because of the quasi-biennial nature of the winds, the interannual variability is very large peaking between 10 and 20 hPa. The SAO wind transition in the upper stratosphere also shows a high amount of interannual variability.



3.3 Agreement Among the REM Members

3.3.1 Temperature

The previous section dealt with the mean of three of the more recent reanalyses (MERRA, ERA-I, and JRA-55). Now we examine their variability or ‘degree of disagreement’ over time. We define the ‘degree of disagreement’ as the standard deviation of the three reanalyses for each month, for each latitude zone, and for each pressure level for the 1979-2014 period. Latitude zones (e.g. 60° - 90° N) are the cosine weighted summations of the 2.5° zonal standard deviations. For some months in the upper stratosphere the temperature disagreement can be greater than 5 K. Figure 4 shows how the monthly temperature disagreement varies in three latitude zones (60°-90° N, 10° S-10° N, and 90°-60° S) in a time versus pressure plot. In all three latitude bands the disagreements are greatest at pressures lower than 10 hPa where there are fewer conventional observations available for assimilation and the satellite observations generally have very broad weighting functions in the vertical. The 60°-90° N plot shows that at pressures greater than 20 hPa level all three reanalyses agree with each other very well, with a standard deviation smaller than 0.5 K. Generally, as time moves forward from 1979 to 2014 the pressure at which the 0.5 K contour occurs moves upward from between 20 and 10 hPa to between 7 and 5 hPa. Interrupting this upward trend is the period during the 1990’s in which the NH polar activity was unusually quiet and cold. (Pawson and Naujokat, 1999, Charlton and Polvani, 2007). The disagreement between the three reanalyses is greater in June-August than in other months.

In the tropics, the disagreement maximizes in two separate layers: between 150 and 70 hPa during the TOVS period (1979-1998), and above 20 hPa throughout the entire 1979-2014 period. The former disagreement is at the vertical location of the cold point temperature. Apparently, there is greater disagreement between the three reanalyses in determining this temperature during the TOVS period than during the ATOVS period. The pressure at which the greatest differences (3-4 K) occur is at 2 hPa.

In the 90°-60° S zone, the disagreement between the three reanalyses extends lower into the stratosphere than the NH polar zone. This region encompasses all of Antarctica and the ocean surrounding it. There are very few observation sites in this latitude zone. Manney et al. (2005) and Lawrence et al. (2015) have shown that reanalyses of temperatures in the polar stratosphere can differ significantly depending on what observations are available. Differences greater than 0.5 K during the TOVS period extend to 70 hPa. There are two layers of greatest disagreement in the TOVS period: between 7 and 5 hPa and above 3 hPa. The disagreement between 7 and 5 hPa terminates with the change from TOVS to ATOVS periods. There is improvement in the differences after 2002 which may be due to the assimilation of AIRS radiances.

3.3.2 Zonal Winds



Figure 5 shows the disagreement of the monthly ensemble members' zonal wind in the polar jet regions (40° - 80° N, and 80° - 40° S) and in the tropics (10° S- 10° N). There is very good agreement of the zonal winds between the three reanalyses in the NH and SH polar jet regions with standard deviations smaller than 0.5 m/s. In the NH polar jet region significant disagreement (>0.5 m/s) between the three reanalyses is consistently confined to pressures lower than 5 hPa. Disagreements greater than 0.5 m/s are nearly eliminated after the transition to ATOVS observations in 1998.

The altitude range of disagreement greater than 0.5 m/s in the SH polar jet region extends from the upper stratosphere down into the middle stratosphere (10-20 hPa) during the TOVS time period, but improve considerably in the ATOVS time period.

The tropical zonal wind disagreement shows much larger values of the order of 10 m/s in the upper stratosphere than the polar jet values, resulting from disagreement in SAO and QBO winds and winds near the surface at 850 hPa. There is improvement with time in the agreement of the QBO winds and 850 winds, but this improvement does not extend to the SAO height region. The greater improvement to the NH and SH polar jet winds after 1998 versus minor improvement of the equatorial winds illustrates the differences between the mechanisms controlling these winds. The polar jet winds are largely dictated by the latitudinal thermal gradient and resulting thermal wind. However, in the tropics the thermal wind relation breaks down and the wind fields are not well constrained by the assimilated satellite radiances. In addition, the tropical winds are primarily determined by the transfer of momentum from upward propagating waves, whose spatial scales are too small to be adequately resolved by the forecast models used in these reanalyses (Baldwin et al., 2001). The tropical winds are therefore highly dependent upon radiosonde observations for speed and direction (and these only extend to ~ 10 hPa). In general the amplitude of the reanalysis tropical winds are smaller than observations. Following the change to ATOVS data, the differences between the reanalyses decrease slightly. None of the forecast models included in the REM are capable of generating a QBO on its own. To date, only the forecast model used in MERRA-2 is capable of doing so, and Coy et al. (2016) show that after 2000 the MERRA-2 QBO winds are greatly improved versus those in MERRA.

4 Intercomparisons of the Reanalyses

In this section we extend our evaluation to the individual reanalyses, and examine how each of eight reanalyses (CFSR, MERRA, ERA-I, JRA-55, MERRA-2, JRA-25, ERA-40, and R-1) differs from the REM for both temperatures and winds. We do not show comparisons of R-2, but one can expect all R-2 qualities to be nearly the same as those of R-1. We also do not show comparisons with the 20CR as that reanalysis assimilated no upper-air observations.



4.1 Temperature

In the left column of Figure 6 the time-mean SH polar (90° - 60° S) zonal mean temperature difference from the REM (Reanalysis – REM) for each month is presented, while the right column shows the time series of the zonal mean monthly mean differences from 1979 through 2014. The left hand column shows the gross monthly mean differences while the right hand column shows the monthly differences over time. Both are useful to illustrate where in the vertical and when in the annual cycle the differences occur and whether these improve over time. Differences in the right column typically do not extend throughout the entire 1979-2014 period. Rather, much like the other differences discussed earlier, large improvements are seen going from the TOVS to ATOVS time periods, with the TOVS time period having the larger differences extending down further from the upper stratosphere into the middle stratosphere. Except where specifically mentioned, temperature differences between the individual reanalysis and the REM are within ± 0.5 K. In general the earlier reanalyses (JRA-25, ERA-40, and R-1) show greater differences from the REM than the more recent reanalyses (CFSR, ERA-I, JRA-55, MERRA, and MERRA-2). Also, in general, the NH and SH polar latitudes show similar difference patterns, with much greater differences in the SH. Thus, in the following, we start with the description on the SH polar latitudes, then mention the NH polar latitudes relatively briefly, and finally describe the equatorial latitudes where the patterns are quite different from those at higher latitudes.

4.1.1. SH polar latitudes

The CFSR temperatures are 6-8 K warmer than the REM in the upper stratosphere peaking during the period of minimum temperatures in that region between March and July. Just below this warm region, there is a small altitude region with colder temperatures than the REM of -1 and -2 K. The time series plot shows that the CFSR's upper stratospheric warm bias occurs throughout the entire 1979-2014 time span with similar seasonal variability

MERRA shows a warm bias of 1 to 2 K in the time-mean plot compared to the REM between 2 and 3 hPa from July through February. Below this, between 5 and 20 hPa, there is a cold bias of -1 to -2 K from April through August. The time series plot shows that this cold bias only exists during the TOVS period, while the warm bias at higher altitudes persists throughout the entire period.

The ERA-I has a mixture of cold (-1 K, March through August) and warm (2 K, November through February) biases compared to the REM between 1 and 3 hPa. An opposite set of biases exist slightly below between 5 and 10 hPa during roughly the same time periods. The time series plot shows that the upper stratosphere cold bias exists during the 1990's. The upper stratosphere warm bias occurs after 1998 while the warm bias between 10 and 5 hPa persists throughout the entire TOVS period.



The JRA-55 shows a year-round cold bias (-2 to -4 K) compared to the REM between 1 and 5 hPa from July through March which then descends to 7 hPa as a warm bias forms between 1 and 2 hPa from March through June. The time series plot shows that temperature differences transitioned from the TOVS to ATOVS period with the cold bias of -4 to -6 K becoming the dominant feature during this latter period.

5 MERRA-2 has a year-round cold bias of -1 to -2 K compared to the REM from 1 to 2 hPa, a year-round warm bias from 3 to 5 hPa, and a cold bias at 10 hPa from March through June. The time series shows that these biases are largest during the TOVS period, with much smaller differences during the ATOVS period and that any bias is greatly reduced after August 2004 when Aura/MLS temperatures at pressures less than 5 hPa are assimilated.

10 The JRA-25 time-mean plot shows greater differences from the REM than the above five reanalyses, with a yearlong warm bias (8 to 10 K) compared to the REM from 1 to 3 hPa and a very cold bias (-4 to -6 K) during the SH winter period between 5 and 10 hPa. In the middle stratosphere there are periods of persistent warm bias with maximum (-2 to -4 K) occurring in the August-November months. The time series plot shows that the upper stratosphere warm bias (8 to 12 K) persists throughout the entire time period, with greater values (>12 K) in the TOVS period. The cold bias (ranging between -2 to -10 K) just below the warm bias occurs mostly during the ATOVS time period. The middle stratosphere cold bias (-2 to
15 -6 K) occurs during the TOVS period (see Section 5.2 of Fujiwara et al., 2017 for its reason).

The ERA-40 time-mean plot shows a strong cold bias (-2 to -6 K) compared to the REM persisting yearlong between 2 and 10 hPa. Just below this is a warm bias (2 to 4 K) between 10-30 hPa. The annual cycle of both the cold bias and warm bias show a slight rising in summer and lowering in winter months. In the lower stratosphere and upper troposphere there are layers and monthly periods of slight cold (> -2 K) and slight warm (< 2 K) bias. The time series plot shows that these
20 biases occur throughout most of the ERA-40 time period which ends in 2002.

R-1 does not analyze at pressures lower than 10 hPa, so there is no evaluation in the upper stratosphere. But there is a nearly year-round warm bias (1 to 2 K) compared to the REM between 10 and 50 hPa peaking between June and September. Another shallow layer of warm bias (1 to 2 K) exists between 100 and 400 hPa. The time series plot shows that the middle stratospheric warm bias is most pronounced in the TOVS period.

25 4.1.2. NH Polar Latitudes

Many features in the upper stratosphere are seasonally common between the NH and SH polar latitudes (Figure 7). However, differences with the REM in the middle and lower stratosphere in the SH are reduced or eliminated in the NH. The CFSR's winter time warm bias that occurs at pressures lower than 7 hPa extends from October through March. There is no evidence of a cold bias underneath this warm bias in the monthly means as occurs in the SH. The time series of
30 differences shows that the differences that occur in the middle and lower stratosphere in the SH do not exist in the NH. MERRA differences from the REM in the NH are much smaller in the monthly means with just a thin warm bias layer



between 3 and 5 hPa. The time series shows only slight differences in the middle and lower stratosphere during the TOVS period compared to the same altitude region in the SH. The ERA-I and JRA-55 have very similar seasonal biases as occurred in the SH. Similar to MERRA, the time series of differences for the ERA-I during the TOVS period in the middle and lower stratosphere are nearly eliminated. The JRA-55 time series does not have noticeable differences from what was observed in the SH. The cold bias that occurred between 10 and 5 hPa in the MERRA-2 differences during the SH winter season is not present in the NH winter differences. The JRA-25, ERA-40, and R-1 all show similar seasonal biases from the REM in the upper stratosphere. Their time series show reduced differences in the middle and lower stratosphere.

4.1.3. Equatorial Latitudes

Differences of reanalysis temperatures from the REM in the equatorial regions (10° S- 10° N) vary more on a semi-annual basis. Figure 8 shows that such is the case for the CFSR's upper stratosphere warm bias of 2 to 4 K and for the JRA-55's upper stratosphere cold bias of -2 to -4 K. The MERRA and ERA-I exhibit a slight warm bias at pressures lower than 5 hPa. The time series plots for the CFSR shows the jumps associated with the different streams and the gradually increasing warm bias in the upper stratosphere during each of these streams. A warm bias centered at 100 hPa, and a cold bias below, persist though the ATOVS period. The MERRA and ERA-I have temperature biases that are greater during the TOVS period than the ATOVS period. In the ATOVS period the bias in both reanalyses is confined to the upper stratosphere at pressures less than 3 hPa with a warm bias of 0.5 to 1 K. The JRA-55 reanalyses shows that the cold biases are nearly constant throughout the entire time series. MERRA-2 shows relatively small differences (< 1 K) at all altitudes compared to the REM and the near elimination of any bias after August 2004 when MLS temperatures at pressures less than 5 hPa were assimilated.

The JRA-25 has a consistent warm bias of 4 to 6 K in the upper stratosphere at pressures less than 3 hPa. Immediately below this is a cold bias of -6 to -8 K that is largest during the ATOVS period. Between 30 and 50 hPa, there is another layer of cold bias of -4 to -6 K that is present only during the TOVS period. ERA-40 has a persistent cold bias of -6 to -8 K in the upper stratosphere between 2 and 7 hPa and two layers of warm bias of 0.5 to 1 K in the middle stratosphere and tropopause regions. R-1 in the middle stratosphere has slight warm and cold biases associated with the QBO (seen in the time series plot). There is also a persistent warm bias of 2 to 4 K in the upper troposphere to tropopause layer between 70 and 200 hPa. This warm bias persists from the TOVS period to the ATOVS period where its magnitude decreases to a warm bias of 1 to 2 K. Randel et al. (2004) pointed this out in their comparison of analyses and attributed the inability to capture lower tropopause temperatures to the coarse vertical resolution and the assimilation of retrieved temperatures (as opposed to radiances).

As discussed in Section 3.3 the three members of the ensemble mean have their greatest disagreement in the upper stratosphere. From the above differences compared to the REM temperatures, the upper stratospheric warm bias of MERRA



and ERA-I at all latitudes is nearly counterbalanced by the cold bias of the JRA-55. The ERA-I warm bias between 5-7 hPa in the SH polar latitudes is counterbalanced somewhat equally by the MERRA and JRA-55 reanalyses.

4.2 Zonal Wind

4.2.1. SH Polar Latitudes

5 The time-mean SH polar jet differences (see Supplement) of the individual reanalyses from the REM are relatively small, ranging from -2 to 1 m/s, with most differences smaller in magnitude than that. As presented in section 3.3.2, the REM members agree quite well in the polar jet region in both hemispheres. Some notable features are as follows. For all reanalyses except R-1, the upper stratosphere is the region where the greatest differences from the REM is seen, but shows much improvement from the TOVS to ATOVS periods. MERRA-2 shows further improvements after 2004 when the MLS
10 temperatures started to be assimilated at pressures less than 5 hPa. JRA-25 and ERA-40 show greater differences compared to more recent reanalyses. Finally, R-1 shows an easterly bias to the westerlies during the transition months from westerlies to easterlies in the middle and lower stratosphere for most of the entire time series.

4.2.2. NH Polar Latitudes

15 Just as with the NH temperatures differences in section 4.1.2, the NH polar jet wind differences from the REM (see Supplement) are smaller in magnitude than the SH differences and are restricted mainly to the upper stratosphere.

4.2.3. Equatorial Latitudes

20 In Figure 9 differences in the stratosphere at pressures less than 7 hPa show how the reanalyses differ from each other in the strength of the westerly and the easterly phases in the SAO region. CFSR and JRA-55 have weaker westerlies and thus have negative biases of greater than -5 m/s during the March-April and September-November westerly periods. They also have positive biases of greater than 3 m/s during the December-February easterly period. MERRA and ERA-I have stronger westerlies and show positive biases of greater than 3 m/s during the March-April and September-November westerly periods. They also have stronger easterlies during the December-February period but differ slightly during the July-August easterly period. This results in the MERRA and ERA-I having negative biases of less than -3 m/s during the former period. The SAO westerlies in MERRA-2 are more than 10 m/s stronger than those in the REM. The time series shows that the stronger
25 westerlies occur primarily during the TOVS period.

MERRA-2 also transitions from QBO westerlies to easterlies more rapidly than the REM during the TOVS period. The time series plots also show where each reanalysis has a slight easterly or westerly bias associated with the phase of the descending QBO winds. The JRA-25 and R-1 show greater differences from the REM than the other reanalyses. R-1 shows a westerly bias of > 4 m/s during the easterly phase of the QBO from 10 hPa down to 100 hPa. This was discussed as well



by Pawson and Fiorino (1998b). The JRA-25 has an easterly bias > 4 m/s during the easterly phase of the QBO from 10 hPa down to 30 hPa. It should be noted that the CFSR used ERA-40 zonal winds as substitute observations between 30° S- 30° N and 1 to 30 hPa from July 1, 1981 to December 31, 1998 (Saha et al., 2010), hence their differences from the REM during that time period and in that pressure range are very similar.

- 5 Interestingly, in Figure 9 there are also sizable differences in the troposphere. The CFSR zonal winds in the tropical upper troposphere during the TOVS years have an easterly bias. This may be associated with the CFSR having a cold bias of about 1 K in the upper troposphere during this time period. The JRA-55 zonal winds have a westerly bias during this time period. The MERRA and ERA-I zonal wind differences in the upper troposphere are no larger than 0.5 m/s. Hence, the differences from the REM show the CFSR has a consistent layer of negative biases of -1 to -2.5 m/s from 50 to 300 hPa. The JRA-55 shows the other extreme of a consistent positive bias of 1 to 2 m/s from 30 to 200 hPa. The time series plots confirm that these upper troposphere zonal wind biases are persistent during the TOVS time period and are reduced in the ATOVS period.

4.2.4. Comparisons with Singapore QBO Winds

- Kawatani et al. (2016) provides a thorough evaluation of the RMS differences of QBO (70-10 hPa) zonal winds between the more recent reanalyses and observations from all the radiosonde sites in the equatorial latitude zone. We will focus just upon comparisons between the reanalyses and zonal winds at Singapore (1° N, 104° E). Correlations between the monthly mean CFSR, MERRA, ERA-I, JRA-55, and MERRA-2 QBO zonal winds (interpolated to Singapore) and the monthly mean radiosonde wind observations at Singapore (obtained from the Free University of Berlin) are mostly above 0.9. More information about how the reanalyses differ from the Singapore winds can be obtained by evaluating the linear slope of their matched monthly winds and their scatter. Figure 10 (a, b, and c) shows the RMS differences of the reanalyses QBO winds and that at Singapore. Comparisons are shown for the entire 1979-2014 period and then divided into the TOVS (1980-1998) and ATOVS (1999-2014) periods. All of the reanalyses' RMS differences improve during the ATOVS period. All of the RMS differences increase from 70 hPa to 10 hPa as does the amplitude of the winds at these levels. The RMS differences decrease by one half to one third from the TOVS to the ATOVS period. Of these five reanalyses the CFSR performs the poorest having higher RMS differences at nearly all pressure levels during all periods. MERRA-2 has the largest RMS differences at 10 hPa during the TOVS period, but improves during the ATOVS period. Coy et al. (2016) explain that during the 1980's and early 1990's that MERRA-2 overemphasized the annual signal. Figure 10 (d, e, and f) shows the slope of the regression line between the individual reanalysis QBO winds and the Singapore QBO winds. The maximum underestimation (slope smaller than 1) at 50 hPa is present in all of the reanalyses. The reanalysis winds and Singapore winds become more similar in strength at lower pressure levels and are closer in strength during the ATOVS period than the TOVS period. The CFSR has consistently weaker winds at all pressure levels during both the TOVS and ATOVS periods. No one reanalysis is better than the others at all QBO levels in either the TOVS or ATOVS periods.



5 Amplitude of Polar Annual Temperature Cycle

Another way to examine the differences between the reanalyses is to compare their annual temperature amplitude (warmest summer month minus coldest winter month) in the polar latitudes. If a reanalysis has a wintertime warm bias or a summertime cold bias then their annual temperature amplitude will be smaller compared to the other reanalyses. Generally, as Figure 2 shows, the summer time temperatures do not vary much from year to year, while the winter time temperatures have greater interannual variability. The mean polar temperatures in Figure 2 indicate which months would likely be used as the warmest and coldest at the various pressure levels. For these differences we use the coldest (warmest) month from November through March and the warmest (coldest) month from May through September for the Northern Hemisphere (Southern Hemisphere). The lower variability of the SH temperatures ensures that the same months are used for the 1979 to 2014 period. However, in the NH the coldest month at a particular pressure level depends upon whether an SSW occurs. In the upper stratosphere, after an SSW the low temperatures following the warming are usually the lowest of the year. Without a warming the lowest temperatures may well have occurred in November or December. In the middle stratosphere the lowest temperatures will usually occur in December. In the lower stratosphere the lowest temperatures will usually occur in December or January. In Figure 11 a time series of the SH and NH polar zone annual temperature amplitudes is presented. In general the SH annual amplitudes in the middle and upper stratosphere are up to 25 K larger than at the same level in the NH, largely because of the persistent and colder SH winters. At pressures greater than 300 hPa temperature amplitudes in the SH are smaller than those in the NH. SH temperature amplitudes increase from 6-12 K in the troposphere to 48-54 K in the middle stratosphere. Maximum amplitudes (54-60 K) in the SH occur above 10 hPa. In the NH polar latitudes the minimal amplitude of 6-12 K occurs at the polar tropopause. Between the surface and the tropopause the temperature amplitude is larger at 18-24 K. Above the tropopause the temperature amplitude increases up to about 5 hPa where the temperature amplitude lies in the 54-60 K range, although the depth of this layer is not nearly as extensive as in the SH polar regions. There is good agreement between these five more recent reanalyses of the years of peak amplitude in the NH polar region upper stratosphere. The peak SH amplitudes of the five reanalyses are in lesser agreement in year and pressure range.

Individually, the five more recent reanalyses agree well with each other from the surface through the lower stratosphere in both hemispheres. However, the ERA-I shows an annual temperature amplitude in the middle stratosphere that is 6-12 K smaller than the other four reanalyses in the SH and about 6 K smaller in the NH polar regions from 1979-2002. The JRA-55 has smaller maximum amplitudes in the SH than the other four reanalyses, which is associated with its low temperature bias in the upper stratosphere, whereas the CFSR tends to have consistently large maximum amplitudes which are associated with its warm bias. However, the CFSR's temperature amplitudes peak at greater pressures in the upper stratosphere and then decreases rapidly between 3 and 1 hPa in both hemispheres, particularly in the ATOVS period. This is most likely due



to the fact that the CFSR did not bias correct the SSU Channel 3 observations and did not assimilate the top AMSU-A channel 14.

As a group the NH plots show that the greatest amplitudes occur at 2 hPa. The years with this large amplitude are years in which an SSW occurred. The years when a SSW did not occur (e.g. the 1990's) have smaller temperature amplitudes in the upper stratosphere. In the SH years in which there was a great amount of wave activity during the winter months had warmer winters and consequently had smaller annual amplitudes. This is particularly noticeably in 2002 and 2010. The ERA-I stands out as having smaller annual amplitudes in the SH middle stratosphere compared to the other four reanalyses during the TOVS period.

6 Comparisons with Satellite Temperature Observations

6.1 HIRDLS and MLS Temperatures

The NASA Earth Observing System (EOS) Aura spacecraft was launched in July 2004 and has onboard several instruments that measure multiple atmospheric constituents. The High Resolution Dynamics Limb Sounder (HIRDLS) (Gille et al., 2008) instrument on the Aura spacecraft made measurements from the upper troposphere through the mesosphere until it prematurely ceased functioning in mid-2008. Quality temperature measurements extend from January 2005 through March 2008. The HIRDLS measurements were not assimilated any of the reanalyses and thus are independent measurements. Monthly mean temperature differences of reanalyses from the HIRDLS (Reanalysis – HIRDLS) temperatures at NH high latitudes (60° - 80° N), tropics (10° S-10° N) and SH high latitudes (60° S) were generated for the 2005 through 2008 period. Figures 12, 13, and 14 present the differences of CFSR, ERA-I, MERRA, JRA-55 and MERRA-2 from the HIRDLS monthly means for these latitude zones, respectively. The time, location and amplitude of the SH differences are generally similar to those of the reanalyses from the REM (Figure 6). The CFSR has a very warm bias of over 14 K in the April to July period at pressures lower than 5 hPa with a cold bias at 7 hPa during this same time period. MERRA has a cold bias of 2 – 4 K from August through April from 1 – 3 hPa and a 2 K warm bias from May through July. ERA-I has a -2 K cold bias at 2 hPa from February through May. JRA-55 has a -4 to -6 K cold bias from July through April between 2 and 3 hPa that become thinner in altitude from April to July as a warm bias occurs from 1 to 2 hPa. MERRA-2 has a warm bias all yearlong at 1 hPa and a -1 to -2 K cold bias from November through March. All of the reanalyses show a slight (< 1 K) warm bias in the middle stratosphere during the November through March period.

In the NH, the CFSR and JRA-55 differences with HIRDLS occur in the same seasons as in the SH with little change in amplitude. The cold bias that MERRA has in the SH does not exist in the NH. The mid-winter warm bias that was in the SH is about a degree warmer in the NH. Similarly, the ERA-I does not have a cold bias in the late winter-spring period, but



there is a warm bias in mid-summer in the upper stratosphere. The cold bias of MERRA-2 in the summer period is smaller in the NH, while the yearlong warm bias exists at 1 hPa. Of interest is that all the reanalyses show a similar warm bias as in the SH during the November through March period.

5 In the tropics, the CFSR has a similar warm bias in a semi-annual basis in the upper stratosphere. MERRA has a warm bias that is highest in altitude during November through February and move lower to 5 to 10 hPa during the other months of the year. ERA-I seems to have a yearlong 0.5 to 1 K warm bias at pressures lower than 10 hPa. JRA-55 has a yearlong -1 to -2 K cold bias between 5 and 2 hPa. MERRA-2 continues to have a yearlong warm bias at 1 hPa and a slight warm bias near 10 hPa.

10 The Microwave Limb Sounder (MLS) is also on the EOS Aura spacecraft. Monthly zonal means of temperatures from the version 4 retrievals were provided by the MLS team for comparisons with reanalyses for the 2005-2014 period. Characteristics of the MLS temperatures are described by Schwartz et al. (2008) and Livesey et al. (2015). Note again that among the reanalyses, MERRA-2 is the only one that assimilated MLS temperatures but only at pressures less than 5 hPa. HIRDLS temperatures have been noted to be colder than the Aura/MLS temperatures (Gille et al., 2008) in the upper
15 temperatures (not shown) are very similar to those with the HIRDLS but less positive. Differences greater than ± 2 K only occur above 10 hPa. Bands of differences of the order of 1 K are present below 10 hPa; however, the MLS documentation notes that there are known oscillations of this magnitude in comparison with other satellite temperature sensors, so these latter differences are not considered significant. Overall differences from the MLS observations are in agreement with the characteristics already described for each of these reanalyses.

20 6.2 Atmospheric Layer Temperature Anomalies

Long-term satellite observations from NOAA polar orbiting satellites of temperatures of the lower stratosphere (TLS) are available from the MSU 4 and AMSU-A 9 microwave channels, while the Stratospheric Sounding Unit channel 1 (SSU1) and channel 2 (SSU2) provide temperature observations of the middle and upper stratosphere, respectively. The satellite weighting functions for these three channels can be found in e.g. Fujiwara et al. (2017, their Fig. 7) and Zou et al. (2014) and
25 on the NOAA/STAR SSU website (<http://www.star.nesdis.noaa.gov/smcd/emb/mscat/index.php>). Zou and Qian (2016) explain the process of merging and extending the infrared based SSU observations with the microwave based AMSU-A and ATMS observations. These satellite-observation climate data records have been used to compare with climate model runs to see if the model is accurately capturing the atmospheric vertical temperature changes since 1979 (Zhao et al., 2016). Other studies use these temperature data records to monitor changes in the Brewer-Dobson Circulation (Young et al., 2011, Young
30 et al., 2012). Randel et al. (2016) compared global and latitudinal trends from SSU with Aura/MLS and SABER



temperatures. Seidel et al. (2016) intercompared the TLS and SSU channel trends from three satellite centers for the entire (1979-2015) period and separate trends for pre-1997 and post-1997. Mitchell et al. (2014) generated TLS, and SSU channel weighted temperatures from reanalyses to see how well they compare with the satellite observations. We perform a similar exercise applying the TLS, SSU1 and SSU2 weights to the reanalyses temperatures at their standard pressure level temperatures. SSU3 layer temperatures were not generated because there were insufficient pressure levels from the majority of the reanalyses to adequately represent this layer. Global mean TLS, SSU1 and SSU2 temperatures are generated for each month from 1979 through 2015. Anomalies from the 1981-2010 period for the TLS, SSU1 and SSU2 are generated. These anomalies are compared against the NOAA/STAR SSU v2.0 data set (Zou et al., 2014) and MSU/AMSU mean layer atmospheric temperature v3.0 (Zou and Wang, 2012). The left column of Figure 15 shows the monthly TLS, SSU1 and SSU2 temperature anomalies, from the CFSR, ERA-I, JRA-55, MERRA, and MERRA-2 from 1979 through 2014 with the NOAA/STAR anomalies overplotted in black. To better assess how each reanalysis differs from the NOAA/STAR anomalies, the right column shows the differences of each reanalysis anomalies from the NOAA/STAR anomalies. The reanalyses TLS anomalies differ from the NOAA/STAR anomalies by less than ± 2.5 K for most of the time series. Most noticeable is that the ERA-I has smaller anomalies than NOAA/STAR in the early 1980's and then has larger anomalies after 2006. Aside from the ERA-I, the other reanalyses seem to agree with the NOAA/STAR anomalies during the El Chichón volcanic period (1982-1984) but with the exception of MERRA and MERRA-2 have smaller anomalies during the Mt. Pinatubo volcanic period (1991-1993). There is a noticeable decrease in the reanalyses anomalies with respect to the NOAA/STAR anomalies in 1999 followed by a gradual increase in time until 2006, after which the reanalyses begin to disagree more with each other. 2006 is when GPSRO observations from the COSMIC constellation became available for assimilation.

The SSU1 temperature anomalies from the CFSR shows large temperature jumps associated with the six streams, preventing any useful evaluation. The other four reanalyses differ from the NOAA/STAR by less than ± 0.5 K for most of the time series. The ERA-I, MERRA, MERRA-2, and JRA-55 all show smaller anomalies than the NOAA/STAR in the early 1980's. There is minor disagreement between the four reanalyses with the NOAA/STAR between the late 1980's through the early 2000's. Beginning in 2006, just as with the TLS anomalies, the disagreement between the four reanalyses increases.

Just as with the SSU1 anomalies, the large temperature jumps associated with the CFSR's stream transitions prevents a proper evaluation of its SSU2 time series. Aside from the CFSR, the other four reanalyses are within ± 0.5 K of the NOAA/STAR anomalies. The JRA-55 matches the NOAA/STAR SSU2 observations very well throughout the entire time series with the exception of a period in the late 1990's and early 2000's when its anomalies are smaller than the NOAA/STAR anomalies. The ERA-I matches the NOAA/STAR SSU2 observations very well except after 2006 when it



exhibits a positive trend. MERRA initially begins with lower SSU2 anomalies than NOAA/STAR, whereas MERRA-2 anomalies are much closer to the NOAA/STAR anomalies. MERRA-2 separates from MERRA after 2005 with more negative anomalies. This is most likely due to the assimilation of MLS temperatures at pressures less than 5 hPa which has shown to produce lower temperatures than before 2005.

5 7 Summary and Conclusions

In this paper a comparison of monthly zonal mean temperatures and zonal winds from the five more recent reanalyses and several older reanalyses were evaluated and intercompared. Our initial evaluation was to look for temperature discontinuities in the time series of each of the reanalyses. This showed that the earlier reanalyses (ERA-40 and JRA-25) had multiple temporal discontinuities in the 1980's in the stratosphere associated with changes in the NOAA TOVS/SSU instruments. The R-1 and R-2 did not show such discontinuities because they used NESDIS-generated temperature profiles, not the original radiance data. NESDIS most likely strived to minimize such discontinuities in their profile temperatures. Almost all the reanalyses have a temporal discontinuity in 1998 when the ATOVS observations became available and the reanalyses either switched immediately from the TOVS to the ATOVS observations or in the case of MERRA and JRA-55 transitioned from the TOVS to the ATOVS over several years. The CFSR has temporal discontinuities at the time of switching from one stream to the next. The CFSR bias-corrected the top SSU channel 3. The model used by the CFSR had a warm bias in the upper stratosphere and slowly warmed about 5 K during the course of each stream. Because of the presence of the discontinuities and transitions discussed above, great caution should be exercised in using reanalyses for trend analysis and/or trend detection, especially in the middle and upper stratosphere.

So as not to favor any one particular reanalysis a reanalysis ensemble mean (REM) of three of the more recent reanalyses (MERRA, ERA-I, and JRA-55) was generated. We presented the climatological mean (1981-2010) of the temperature and zonal wind REM and showed the altitudes and seasons with the largest variance in the REM. The temperature and zonal winds have greatest interannual variability in the NH polar region from January through March because of the large variability in wave activity, including the frequent occurrence of strong stratospheric warming events. This variability is greatest in the upper stratosphere as planetary-scale wave-amplitudes, and the associated temperature and zonal wind changes, during strong stratospheric warming events are largest in the upper stratosphere. In the SH polar region the interannual variability is not as large in magnitude and is prevalent throughout the stratosphere. Because mid-winter wave activity is much smaller in the SH, most of the interannual variability in the SH polar region is associated with the springtime transition to summer circulation patterns and polar vortex breakdown, when wave activity show larger interannual variability in timing and magnitude.



Time series of the temperature variance of the three REM members showed that the greatest disagreement occurs during the TOVS time period (1979-1998) in all three latitude zones and agreement improves during the ATOVS time period (1999 to present). The disagreement in the SH polar latitudes extended lower into the stratosphere than in the NH polar latitudes. The zonal wind variance was smaller than the temperature variance in the polar latitudes, but had a similar temporal
5 difference between the TOVS and ATOVS time periods. In the tropics, the zonal wind variance was much larger than in the polar regions as the disagreement of the SAO and QBO zonal winds was quite large. Thus, improving equatorial winds in future reanalyses is an important goal.

The characteristics of each reanalysis were identified as differences from the temperature and zonal wind REM. The CFSR had a warm bias compared to the REM in the upper stratosphere that occurred through all four seasons and persisted during
10 both the TOVS and ATOVS time periods. The JRA-55, on the other hand, had a cold bias that occurred through all four seasons and persisted during both the TOVS and ATOVS time periods. ERA-I and MERRA had smaller differences from the temperature REM except that the ERA-I had a warm bias in the SH polar latitudes between 7 and 5 hPa that occurred only during the austral winter and only during the TOVS time period. MERRA-2 had very small differences from the REM
15 except in the upper stratosphere in the polar regions where it had a yearlong warm bias at 1 hPa and cool bias between 2-3 hPa. These biases greatly diminished during the ATOVS period. Temperature differences from the REM in the earlier reanalyses (JRA-25, ERA-40, and R-1) extended throughout the stratosphere and the upper troposphere. These differences occurred through both the TOVS and ATOVS time periods.

In the tropics, the individual reanalyses exhibited smaller temperature differences than in the polar latitudes. But the characteristic biases in the upper stratosphere observed in the polar latitudes were maintained in the tropics. The zonal wind
20 differences from the REM of the individual reanalyses are very large in the SAO region. In the QBO region the differences frequently show differences in the timing of the descending westerlies and easterlies as well as the amplitude of these winds. Zonal wind differences from the REM were not confined to the stratosphere as several reanalyses also had sizable differences in the troposphere.

Specifically comparing the more recent reanalyses QBO zonal winds (70-10 hPa) against the zonal winds observed at
25 Singapore using the FUB data set showed that the CFSR had the largest RMS differences from the Singapore winds than the other reanalyses at most levels and during both the TOVS and ATOVS periods. However, MERRA-2 10 hPa zonal winds were nearly twice as large as the other reanalyses during the TOVS period. The RMS differences from the Singapore zonal winds were smaller during the ATOVS period for all the reanalyses. The CFSR had the largest amplitude biases from the Singapore winds as shown by the linear slope of their matched monthly values. The linear slopes of all the reanalyses were
30 furthest from unity at 50 and 30 hPa during the TOVS period than the ATOVS period.



The amplitude of the annual temperature cycle (warmest summer month minus the coldest winter month) in the SH polar latitudes is larger than the NH polar latitude temperature amplitude by 6-12 K. The region of large amplitude extends throughout the middle and upper stratosphere in the SH polar latitude. In the NH polar latitudes the vertical region of large temperature amplitudes is confined to the upper stratosphere and occurs during the years with an SSW. The ERA-I has a noticeably smaller annual temperature amplitude in the SH polar latitudes than the other ensemble members from 3 to 30 hPa. This is due to its warm bias during the SH winter months in this latitude region. The CFSR's temperature amplitude decreases rapidly above 3 hPa due to its warm bias in the upper stratosphere in both SH and NH polar latitudes. Comparisons against HIRDLS (January 2005-March 2008) and Aura/MLS (2005-2014) temperatures concur with previous characteristics of the various reanalyses in the upper stratosphere. The CFSR has a definite warm bias compared to HIRDLS temperatures while the JRA-55 has a definite cold bias. Both MERRA and ERA-I have a slight warm bias during the summer months between 3 – 7 hPa. MERRA has a slight cold bias above this between 1 and 2 hPa nearly all year long. MERRA-2 assimilates Aura/MLS temperatures at pressures less than 5 hPa and consequently differences are very small.

In this paper we have examined the thermal and dynamical characteristics of the older as well as the more recent reanalyses. We find that the more recent reanalyses have fewer discontinuities in their temperature and wind time series due to better data assimilation techniques and transition between different sets of observations. We also find that the larger temperature and wind differences between the older reanalyses have become smaller between the more recent reanalyses. However, the transition from the TOVS to ATOVS satellite periods continues to be problematic. The reanalysis QBO winds during the ATOVS period also agree much better with the Singapore radiosonde observations than during the TOVS period. We expect that future reanalyses will have better QBO winds as their forecast models improve to produce a spontaneous QBO in the tropics. We have shown that the more recent reanalysis agree quite well with each other in the lower and middle stratosphere, but greater differences exist in the upper stratosphere and lower mesosphere. This latter disagreement is a result of differences in model top and vertical resolution and what data is assimilated. Due to these disagreements we caution data users from using any one reanalysis for comparisons and even more so for detection of trends and or changes in climate.

25 **Appendix A: Major abbreviations and terms**

20CR: 20th Century Reanalysis of NOAA and CIRES

ATOVS: Advanced TIROS Operational Vertical Sounder

AMSU: Advanced Microwave Sounding Unit (AMSU-A for Unit A)

Aura: a satellite in the EOS A-Train satellite constellation

30 CIRA86: COSPAR International Reference Atmosphere, 1986

CIRES: Cooperative Institute for Research in Environmental Sciences (NOAA and University of Colorado Boulder)



- CFSR: Climate Forecast System Reanalysis of NCEP
COSMIC: Constellation Observing System for Meteorology, Ionosphere, and Climate
COSPAR: Committee on Space Research
DOE: Department of Energy
- 5 ECMWF: European Centre for Medium-Range Weather Forecasts
EOS: NASA's Earth Observing System
ERA-15: ECMWF 15-year reanalysis
ERA-40: ECMWF 40-year reanalysis
ERA-I or ERA-Interim: ECMWF interim reanalysis
- 10 GPSRO: Global Positioning System radio occultation
HIRDLS: High Resolution Dynamics Limb Sounder
JRA-25: Japanese 25-year Reanalysis
JRA-55: Japanese 55-year Reanalysis
MERRA: Modern Era Retrospective-Analysis for Research (MERRA-2 for its version 2)
- 15 MLS: Microwave Limb Sounder
MSU: Microwave Sounding Unit
NASA: National Aeronautics and Space Administration
NCAR: National Center for Atmospheric Research
NCEP: National Centers for Environmental Prediction of the NOAA
- 20 NESDIS: National Environmental Satellite, Data, and Information Service of the NOAA
NH: Northern Hemisphere
NOAA: National Oceanic and Atmospheric Administration
NOAA-* (where * is number): NOAA's polar-orbiting operational meteorological satellite, number *
QBO: quasi-biennial oscillation
- 25 R-1: NCEP-NCAR Reanalysis 1
R-2: NCEP-DOE Reanalysis 2
REM: Reanalysis Ensemble Mean
RMS: root mean square
S-RIP: SPARC Reanalysis Intercomparison Project
- 30 SAO: semi-annual oscillation
SH: Southern Hemisphere



SPARC: Stratosphere–troposphere Processes And their Role in Climate

SSU: Stratospheric Sounding Unit (SSU1 and SSU2 for SSU Channel 1 and 2, respectively)

SSW: Sudden Stratospheric Warming

STAR: Center for Satellite Applications and Research of the NESDIS

5 TIROS: Television Infrared Observation Satellite

TLS: temperature of the lower stratosphere (MSU channel 4 / AMSU channel 9)

TOVS: TIROS Operational Vertical Sounder

WMO: World Meteorological Organization

10

Acknowledgements. We acknowledge the scientific guidance and sponsorship of the World Climate Research Programme, coordinated in the framework of SPARC. We are grateful for the internal reviews, alterations, and improvements by two of the S-RIP co-leads Gloria L. Manney and Lesley J. Gray. We thank the reanalysis centres for providing their support and data products. We thank Michael Schwartz for providing the MLS monthly temperature data. Masatomo Fujiwara's contribution was financially supported in part by the Japanese Ministry of Education, Culture, Sports, Science and Technology (MEXT) through Grants-in-Aid for Scientific Research (26287117 and 16K05548), and Corwin Wright's by NERC grant NE/K015117/1.

15

References

- 20 Baldwin, M. P., Gray, L.J., Dunkerton, T.J., Hamilton, K., Haynes, P.H., Randel, W.J., Holton, J.R., Alexander, M.J., Hirota, I., Horinouchi, T., Jones, D.B.A., Kinnersley, J.S., Marquardt, C., Sato, K., Takahashi, M.: The quasi-biennial oscillation, *Rev. Geophys.*, 39(2), 179–229, doi:10.1029/1999RG000073, 2001.
- Baldwin, M. and Gray, L.J.: Tropical stratospheric zonal winds in ECMWF ERA-40 reanalysis, rocketsonde data and rawinsonde data. *Geophys. Res. Lett.*, 32 (9), 2005
- 25 Bosilovich, M., Akella, S., Coy, L., Cullather, R., Draper, C., Gelaro, R., Kovach, R., Liu, Q., Molod, A., Norris, P., Wargan, K., Chao, W., Reichle, R., Takacs, L., Vikhliav, Y., Bloom, S., Collow, A., Firth, S., Labow, G., Partyka, G., Pawson, S., Reale, O., Schubert, S. D., and Suarez, M.: MERRA-2: Initial evaluation of the climate, NASA Tech. Rep. Series on Global Modeling and Data Assimilation, NASA/TM–2015-104606, Vol. 43, 2015.
- Charlton, A. J., and Polvani, L. M.: A new look at stratospheric sudden warmings. Part I: Climatology and modelling benchmarks. *J. Climate*, 20, 449–469, doi:10.1175/JCLI3996.1, 2007.
- 30 Compo, G. P., Whitaker, J. S., Sardeshmukh, P. D., Matsui, N., Allan, R. J., Yin, X., Gleason, B. E., Vose, R. S., Rutledge, G., Bessemoulin, P., Brönnimann, S., Brunet, M., Crouthamel, R. I., Grant, A. N., Groisman, P. Y., Jones, P. D., Kruk,



- M. C., Kruger, A. C., Marshall, G. J., Maugeri, M., Mok, H. Y., Nordli, Ø., Ross, T. F., Trigo, R. M., Wang, X. L., Woodruff, S. D., and Worley, S. J.: The twentieth century reanalysis project, *Q. J. Roy. Meteor. Soc.*, 137, 1–28, doi:10.1002/qj.776, 2011.
- 5 Coy, L., K. Wargan, Molod, A. M., McCarty, W. R., and Pawson, S.: Structure and dynamics of the quasi-biennial oscillation in MERRA-2, *J. Clim.*, 29, 5339–5354, doi:10.1175/JCLI-D-15-0809.1, 2016.
- Dee, D. P., Uppala, S. M., Simmons, A. J., Berrisford, P., Poli, P., Kobayashi, S., Andrae, U., Balmaseda, M. A., Balsamo, G., Bauer, P., Bechtold, P., Beljaars, A. C. M., van de Berg, L., Bidlot, J., Bormann, N., Delsol, C., Dragani, R., Fuentes, M., Geer, A. J., Haimberger, L., Healy, S. B., Hersbach, H., Hólm, E. V., Isaksen, I., Kållberg, P., Köhler, M., Matricardi, M., McNally, A. P., Monge-Sanz, B. M., Morcrette, J.-J., Park, B.-K., Peubey, C., de Rosnay, P., Tavolato, C., Thépaut, J.-N., and Vitart, F.: The ERA-Interim reanalysis: configuration and performance of the data assimilation system, *Q. J. Roy. Meteor. Soc.*, 137, 553–597, doi:10.1002/qj.828, 2011.
- 10 Fujiwara, M., Hibino, T., Mehta, S. K., Gray, L., Mitchell, D., and Anstey, J.: Global temperature response to the major volcanic eruptions in multiple reanalysis data sets, *Atmospheric Chemistry and Physics*, 15, 13507–13518, doi:10.5194/acp-15-13507-2015, 2015.
- 15 Fujiwara, M., Wright, J. S., Manney, G. L., Gray, L. J., Anstey, J., Birner, T., Davis, S., Gerber, E. P., Harvey, V. L., Hegglin, M. I., Homeyer, C. R., Knox, J. A., Krüger, K., Lambert, A., Long, C. S., Martineau, P., Molod, A., Monge-Sanz, B. M., Santee, M. L., Tegtmeier, S., Chabrillat, S., Tan, D. G. H., Jackson, D. R., Polavarapu, S., Compo, G. P., Dragani, R., Ebisuzaki, W., Harada, Y., Kobayashi, C., McCarty, W., Onogi, K., Pawson, S., Simmons, A., Wargan, K., Whitaker, J. S., and Zou, C.-Z.: Introduction to the SPARC Reanalysis Intercomparison Project (S-RIP) and overview of the reanalysis systems, *Atmos. Chem. Phys.*, 17, 1417–1452, doi:10.5194/acp-17-1417-2017, 2017.
- 20 Gille, J., Barnett, J., Arter, P., Barker, M., Bernath, P., Boone, C., Cavanaugh, C., Chow, J., Coffey, M., Craft, J., Craig, C., Dials, M., Dean, V., Eden, T., Edwards, D.P., Francis, G., Halvorson, C., Harvey, L., Hepplewhite, C., Khosravi, R., Kinnison, D., Krinsky, C., Lambert, A., Lee, H., Lyjak, L., Loh, J., Mankin, W., Massie, S., McInerney, J., Moorhouse, J., Nardi, B., Packman, D., Randall, C., Reburn, J., Rudolf, W., Schwartz, M., Serafin, J., Stone, K., Torpy, B., Walker, K., Waterfall, A., Watkins, R., Whitney, J., Woodard, D., and Young, G.: High Resolution Dynamics Limb Sounder: Experiment overview, recovery, and validation of initial temperature data, *J. Geophys. Res.*, 113, D16S43, doi:10.1029/2007JD008824, 2008.
- 25 Gibson, J. K., Kållberg, P., Uppala, S. M., Nomura, A., Hernandez, A., and Serrano, E.: ERA description. ERA-15 Rep. Series 1, 72 pp., 1997.
- 30 Kalnay, E., Kanamitsu, M., Kistler, R., Collins, W., Deaven, D., Gandin, L., Iredell, M., Saha, S., White, G., Woollen, J., Zhu, Y., Leetmaa, A., Reynolds, R., Chelliah, M., Ebisuzaki, W., Higgins, W., Janowiak, J., Mo, K. C., Ropelewski, C.,



- Wang, J., Jenne R., and Joseph, D.: The NCEP/NCAR 40-year reanalysis project, *B. Am. Meteorol. Soc.*, 77, 437–471, 1996.
- Kanamitsu, M., Ebisuzaki, W., Woollen, J., Yang, S.-K., Hnilo, J. J., Fiorino, M., and Potter, G. L.: NCEP–DOE AMIP-II reanalysis (R-2), *B. Am. Meteorol. Soc.*, 83, 1631–1643, 2002.
- 5 Kawatani, Y., Hamilton, K., Miyazaki, K., Fujiwara, M., and Anstey, J.: Representation of the tropical stratospheric zonal wind in global atmospheric reanalyses, *Atmospheric Chemistry and Physics*, doi:10.5194/acp-2016-76, 2016.
- Kistler, R., Collins, W., Saha, S., White, G., Woollen, J., Kalnay, E., Chelliah, M., Ebisuzaki, W., Kanamitsu, M., Kousky, V., van den Dool, H., Jenne, R., and Fiorino, M.: The NCEP–NCAR 50-year reanalysis: monthly means CD-ROM and documentation, *B. Am. Meteorol. Soc.*, 82, 247–267, 2001.
- 10 Kobayashi, S., Ota, Y., Harada, Y., Ebata, A., Moriya, M., Onoda, H., Onogi, K., Kamahori, H., Kobayashi, C., Endo, H., Miyaoka, K., and Takahashi, K.: The JRA-55 reanalysis: general specifications and basic characteristics, *J. Meteorol. Soc. Jpn.*, 93, 5–48, doi:10.2151/jmsj.2015-001, 2015. Lawrence, Z. D., Manney, G. L., Minschwaner, K., Santee, M. L., and Lambert, A.: Comparisons of polar processing diagnostics from 34 years of the ERA-Interim and MERRA reanalyses, *Atmos. Chem. Phys.*, 15, 3873–3892, doi:10.5194/acp-15-3873-2015, 2015.
- 15 Livesey, N. J., et al.: EOS MLS version 4.2x level 2 data quality and description document, Tech. Rep. D-33509 Rev. A, Jet Propul. Lab., Calif. Inst. of Technol., Pasadena, Calif., 2015.
- Manney, G. L., Sabutis, J. L., Pawson, S., Santee, M. L., Naujokat, B., Swinbank, R., Gelman, M. E., and Ebisuzaki, W.: Lower stratospheric temperature differences between meteorological analyses in two cold Arctic winters and their impact on polar processing studies, *J. Geophys. Res.*, 108(D5), 8328, doi:10.1029/2001JD001149, 2003.
- 20 Manney, G.L., Allen, D.R., Kruger, K., Naujokat, B., Santee, M.L., Sabutis, J.L., Pawson, S., Swinbank, R., Randall, C.E., Simmons, A.J., and Long, C., "Diagnostic comparison of meteorological analyses during the 2002 Antarctic winter," *Monthly Weather Review* 133, 1261-1278, doi:10.1175/MWR2926.1, May 2005.
- Manney, G.L., Hegglin, M.I., Daffer, W.H., Schwartz, M.J., Santee, M.L., and Pawson, S., "Climatology of Upper Tropospheric/Lower Stratospheric UTLS Jets and Tropopause in MERRA," *J. Climate* 27, 3248-3271, doi:10.1175/JCLI-D-13-00243.1, 2014.
- 25 Martineau, P., and Son, S.-W.: Quality of reanalysis data during stratospheric vortex weakening and intensification events, *Geophys. Res. Lett.*, 37, L22801, doi:10.1029/2010GL045237, 2010.
- Martineau, P., Son, S.-W., and Taguchi, M.: Dynamical Consistency of Reanalysis Datasets in the extratropical Stratosphere, *J. Climate*, 29, 3057-3074, doi: 10.1175/JCLI-D-15-0469.1, 2016.



- Mitchell, D. M., Gray, L. J., Fujiwara, M., Hibino, T., Anstey, J. A., Ebisuzaki, W., Harada, Y., Long, C., Misios, S., Stott, P. A. and Tan, D.: Signatures of naturally induced variability in the atmosphere using multiple reanalysis datasets. *Q. J. R. Meteorol. Soc.*, 141, 2011–2031, doi: 10.1002/qj.2492, 2015.
- Onogi, K., Tsutsui, J., Koide, H., Sakamoto, M., Kobayashi, S., Hatsushika, H., Matsumoto, T., Yamazaki, N., Kamahori, H.,
5 Takahashi, K., Kadokura, S., Wada, K., Kato, K., Oyama, R., Ose, T., Mannoji, N., and Taira, R.: The JRA-25 reanalysis, *J. Meteorol. Soc. Jpn.*, 85, 369–432, doi:10.2151/jmsj.85.369, 2007.
- Pawson, S. and Fiorino, M.: A comparison of reanalyses in the tropical stratosphere: Part 1: thermal structure and the annual cycle, *Clim. Dynam.*, 14, 631–644, 1998a.
- Pawson, S. and Fiorino, M.: A comparison of reanalyses in the tropical stratosphere: Part 2: the quasi-biennial oscillation,
10 *Clim. Dynam.*, 14, 645–658, 1998b.
- Pawson, S. and Fiorino, M.: A comparison of reanalyses in the tropical stratosphere: Part 3: inclusion of the pre-satellite data era, *Clim. Dynam.*, 15, 241–250, 1999.
- Pawson, S., Labitzke, K., Lenschow, R., Naujokat, B., Rajewski, B., Wiesner, M. and Wohlfart, R.-C.: Climatology of the
15 Northern Hemisphere Stratosphere Derived from Berlin Analyses. Part 1: Monthly Means. *Meteorologische Abhandlung, Institut für Meteorologie der F. U. Berlin, Serie A, Band 7, Heft 3*, 1993.
- Pawson, S., and Naujokat, B.: The cold winters of the middle 1990s in the northern lower stratosphere, *J. Geophys. Res.*, 104(D12), 14209–14222, doi:10.1029/1999JD900211, 1999.
- Randel, W., et al.: The SPARC intercomparison of middle-atmosphere climatologies, *J. Climate*, 17, 986–1003, 2004.
- Randel, W., Smith, A.K., Wu, F., Zou, C.-Z., Qian, H., Stratospheric temperature trends over 1979-2015 derived from
20 combined SSU, MLS, and SABER satellite observations, *J. Climate*, 29, 4843-4858, DOI: 10.1175/JCLI-D-15-0629.1, 2016.
- Ray, E. A., Alexander, M. J., and Holton, J. R.: An analysis of the structure and forcing of the equatorial semiannual oscillation in zonal wind, *J. Geophys. Res.*, 103(D2), 1759–1774, doi:10.1029/97JD02679, 1998.
- Rienecker, M. M., Suarez, M. J., Gelaro, R., Todling, R., Bacmeister, J., Liu, E., Bosilovich, M. G., Schubert, S. D., Takacs,
25 L., Kim, G.-K., Bloom, S., Chen, J., Collins, D., Conaty, A., da Silva, A., Gu, W., Joiner, J., Koster, R. D., Lucchesi, R., Molod, A., Owens, T., Pawson, S., Pegion, P., Redder, C. R., Reichle, R., Robertson, F. R., Ruddick, A. G., Sienkiewicz, M., and Woollen, J.: MERRA: NASA’s modern-era retrospective analysis for research and applications, *J. Climate*, 24, 3624–3648, doi:10.1175/JCLI-D-11-00015.1, 2011.
- Saha, S., Moorthi, S., Pan, H.-L., Wu, X., Wang, J., Nadiga, S., Tripp, P., Kistler, R., Woollen, J., Behringer, D., Liu, H.,
30 Stokes, D., Grumbine, R., Gayno, G., Wang, J., Hou, Y.-T., Chuang, H.-Y., Juang, H.-M. H., Sela, J., Iredell, M., Treadon, R., Kleist, D., van Delst, P., Keyser, D., Derber, J., Ek, M., Meng, J., Wei, H., Yang, R., Lord, S., van den



- Dool, H., Kumar, A., Wang, W., Long, C., Chelliah, M., Xue, Y., Huang, B., Schemm, J.-K., Ebisuzaki, W., Lin, R., Xie, P., Chen, M., Zhou, S., Higgins, W., Zou, C.-Z., Liu, Q., Chen, Y., Han, Y., Cucurull, L., Reynolds, R. W., Rutledge, G., and Goldberg, M.: The NCEP climate forecast system reanalysis, *B. Am. Meteorol. Soc.*, 91, 1015–1057, doi:10.1175/2010BAMS3001.1, 2010.
- 5 Schwartz, M. J., et al.: Validation of the Aura Microwave Limb Sounder temperature and geopotential height measurements, *J. Geophys. Res.*, 113, D15S11, doi:10.1029/2007JD008783, 2008.
- Seidel, D. J., J. Li, C. Mears, I. Moradi, J. Nash, W. J. Randel, R. Saunders, D. W. J. Thompson, and C.-Z. Zou: Stratospheric temperature changes during the satellite era, *J. Geophys. Res. Atmos.*, 121, doi:10.1002/2015JD024039, 2016
- 10 Simmons, A. J., Poli, P., Dee, D. P., Berrisford, P., Hersbach, H., Kobayashi, S. and Peubey, C.: Estimating low-frequency variability and trends in atmospheric temperature using ERA-Interim. *Q.J.R. Meteorol. Soc.*, 140: 329–353. doi:10.1002/qj.2317, 2014.
- SPARC : SPARC intercomparison of middle atmosphere climatologies. SPARC Rep. 3, 96 pp., 2002.
- Uppala, S. M., Kållberg, P. W., Simmons, A. J., Andrae, U., Bechtold, V. D. C., Fiorino, M., Gibson, J. K., Haseler, J., 15 Hernandez, A., Kelly, G. A., Li, X., Onogi, K., Saarinen, S., Sokka, N., Allan, R. P., Andersson, E., Arpe, K., Balmaseda, M. A., Beljaars, A. C. M., Berg, L. V. D., Bidlot, J., Bormann, N., Caires, S., Chevallier, F., Dethof, A., Dragosavac, M., Fisher, M., Fuentes, M., Hagemann, S., Hólm, E., Hoskins, B. J., Isaksen, L., Janssen, P. A. E. M., Jenne, R., McNally, A. P., Mahfouf, J.-F., Morcrette, J.-J., Rayner, N. A., Saunders, R. W., Simon, P., Sterl, A., Trenberth, K. E., Untch, A., Vasiljevic, D., Viterbo, P., and Woollen, J.: The ERA-40 reanalysis, *Q. J. Roy. Meteor.* 20 *Soc.*, 131, 2961–3012, doi:10.1256/qj.04.176, 2005.
- Young, P.J., Thompson, D.W.J., Rosenlof, K.H., Solomon, S., Lamarque, J. The seasonal cycle and interannual variability in stratospheric temperatures and links to the Brewer–Dobson circulation: An analysis of MSU and SSU Data. *J. Clim.*, 24, 6243–6258, 2011.
- Young, P.J., Rosenlof, K.H., Solomon, S., Sherwood, S.C., Fu, Q., Lamarque, J-F.: Changes in Stratospheric Temperatures 25 and Their Implications for Changes in the Brewer–Dobson Circulation, 1979–2005. *Journal of Climate* 25:5, 1759–1772, 2012.
- Zhao, L.; Xu, J.; Powell, A.M.; Jiang, Z.; Wang, D. Use of SSU/MSU Satellite Observations to Validate Upper Atmospheric Temperature Trends in CMIP5 Simulations. *Remote Sens.* 2016, 8, 13.
- Zou, C.-Z. and Wang, W.: MSU/AMSU Radiance Fundamental Climate Data Record Calibrated Using Simultaneous Nadir 30 Overpasses Climate Algorithm Theoretical Basis Document (C-ATBD), NOAA/NESDIS, 2012.



Zou, C.-Z., Qian, H., Wang, W., Wang, L., and Long, C.: Recalibration and merging of SSU observations for stratospheric temperature trend studies, *J. Geophys. Res. Atmos.*, 119, 13,180-13,205, doi:10.1002/2014JD021603, 2014.

Zou, C.-Z., Qian, H.: Stratospheric temperature climate data record from merged SSU and AMSU-A observations, *J. Atmos. Oceanic Technology*, 33, 1967-1984, doi:10.1175/JTECH-D-16-0018.1, 2016.

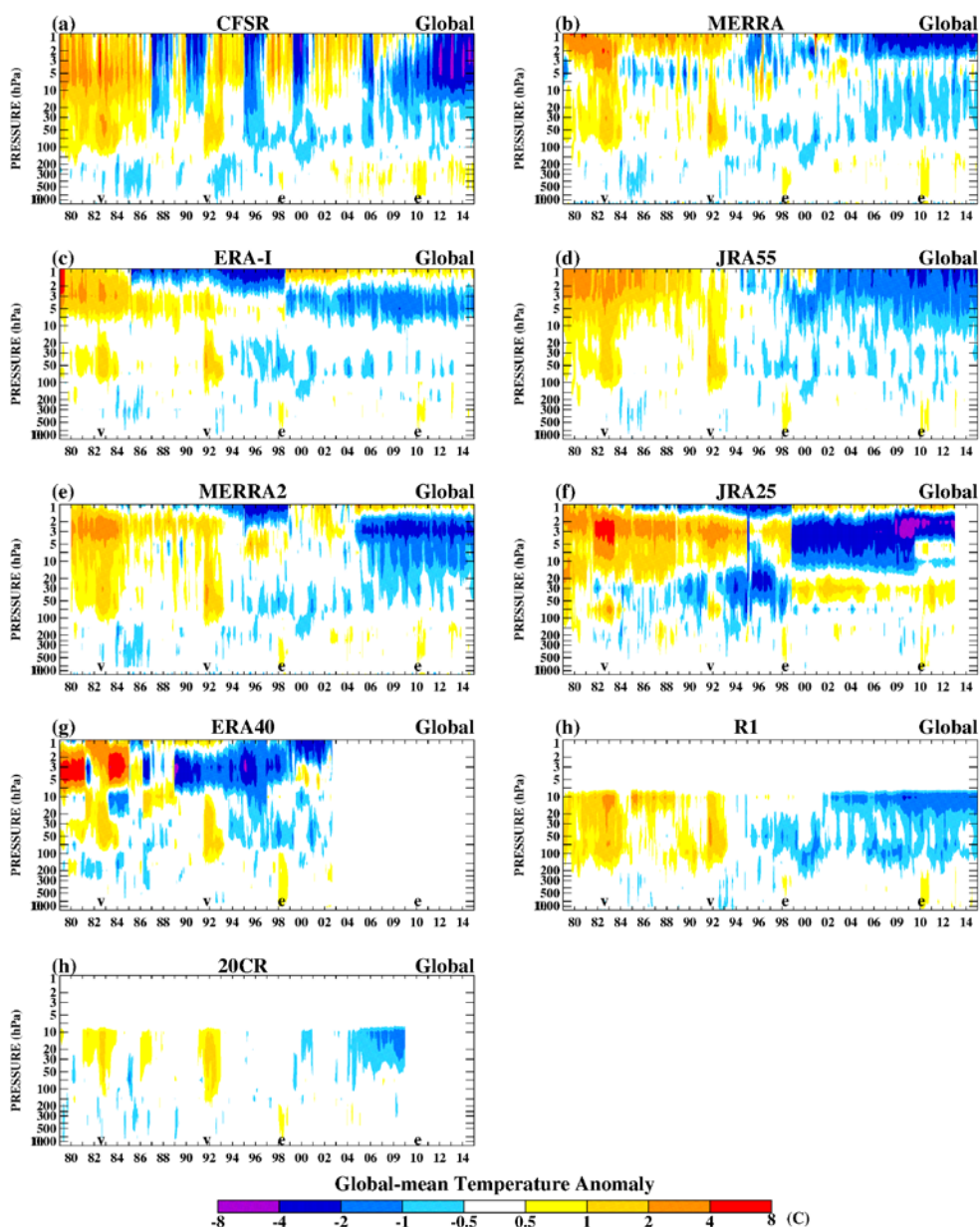


Figure 1. Pressure vs time plots of the global mean temperature anomalies (K) of reanalyses. The anomalies are from each reanalysis' monthly climatology. The reanalyses shown are a)CFSR, b) MERRA, c) ERA-Interim, d) JRA-55, e) MERRA-2, f) ERA-40, g) JRA-25, h) R-1, i) 20CR. Note that R-1 and 20CR do not provide analyses above 10 hPa. “v”s and “e”s denote the occurrence of volcanos and El Ninios.

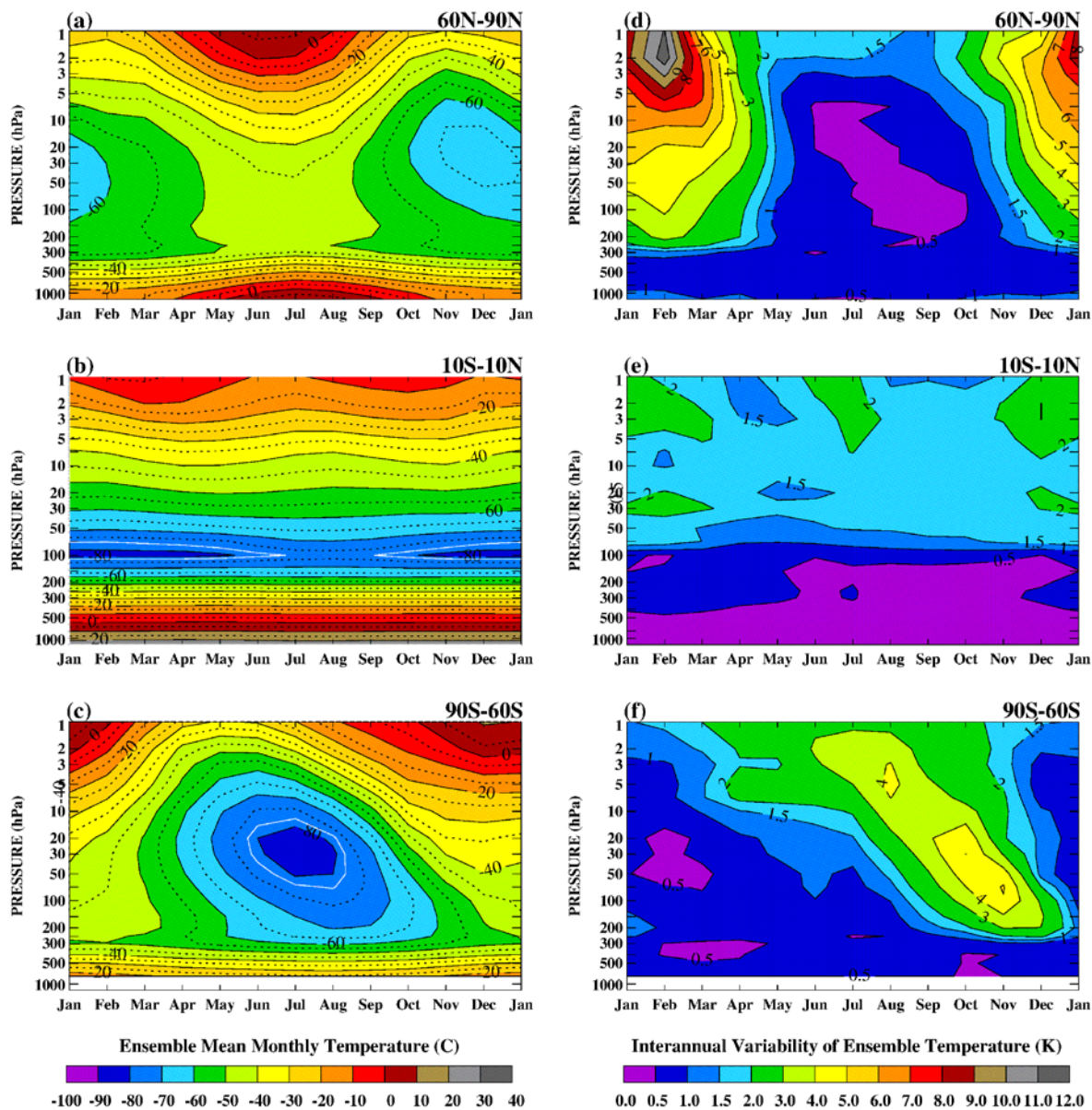


Figure 2. Annual variation of the REM temperature monthly means ($^{\circ}\text{C}$) and their standard deviation (K) in three different zonal regions: 60° - 90° N (top); 10° S - 10° N (middle); and 90° - 60° S (bottom).

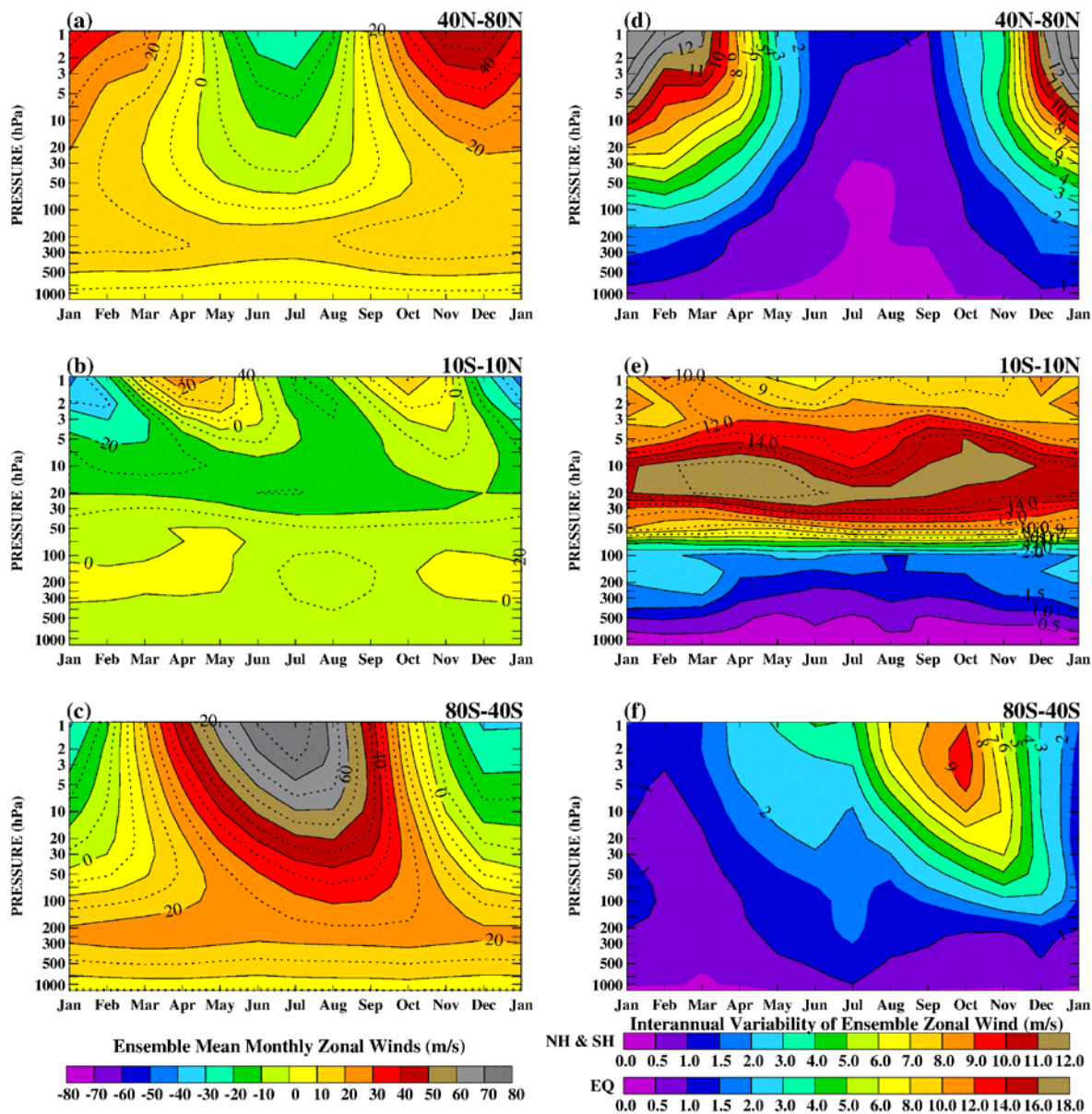


Figure 3. Annual variation of the REM zonal wind monthly means (m/s) and their standard deviation (m/s) in three different zonal regions: 40° - 80° N (top); 10° S - 10° N (middle); and 80° - 40° S (bottom).

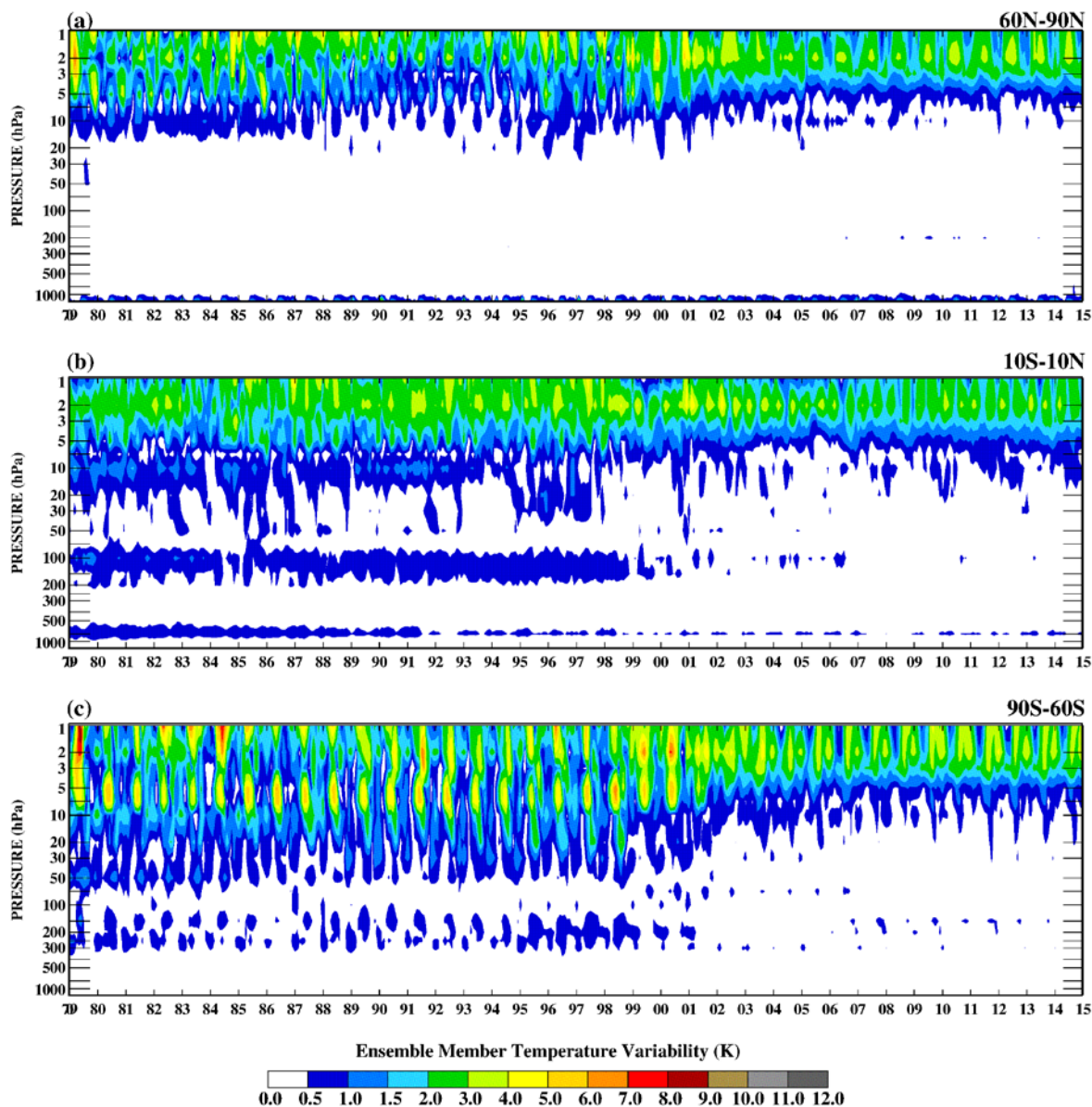


Figure 4. Pressure vs time plots of the temperature standard deviation(K) for each month of the three reanalyses making up the REM for three zonal regions: 60°-90° N (top); 10° S-10° N (middle); and 90°-60°S (bottom).

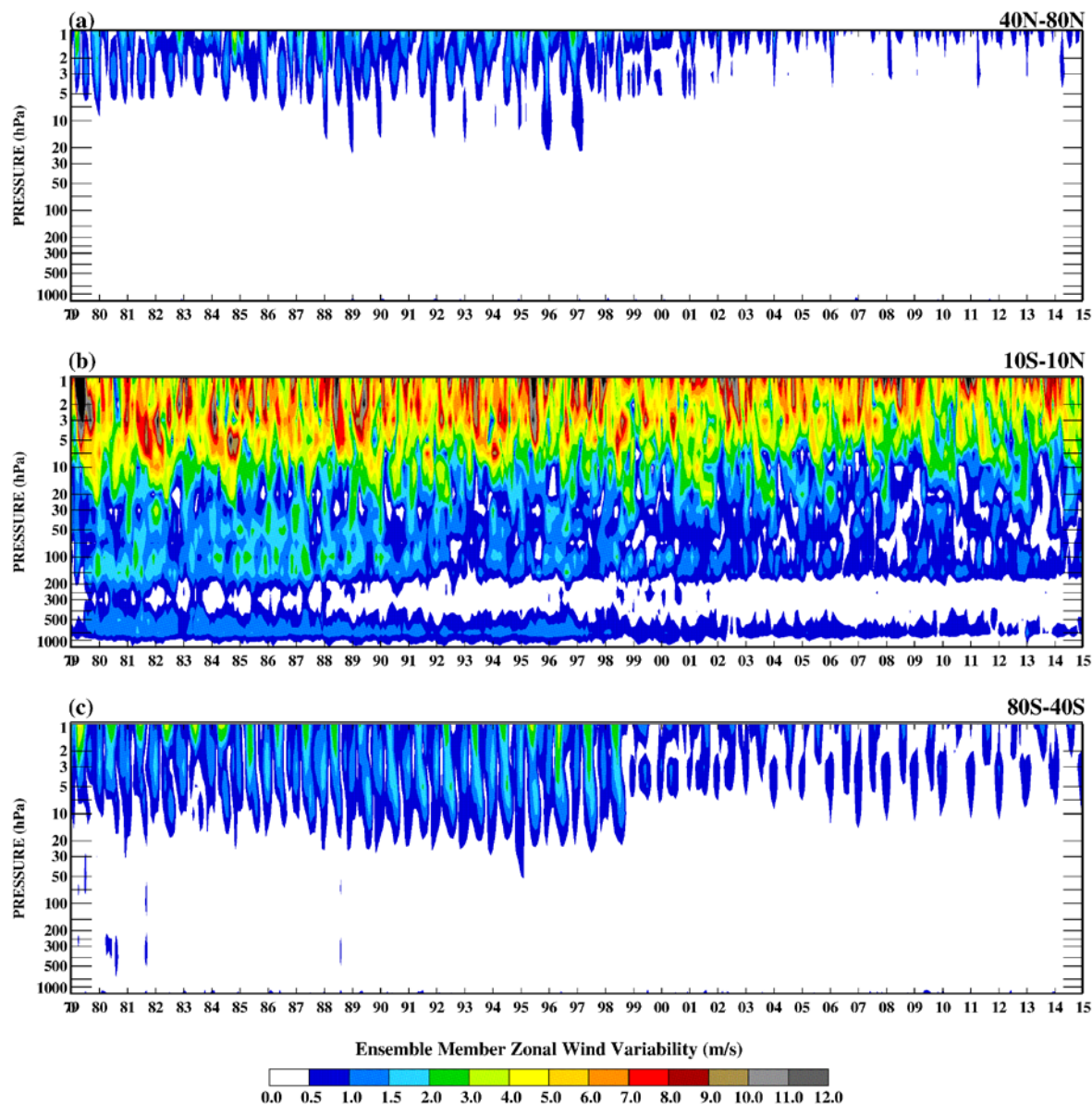


Figure 5. Pressure vs time plots of the zonal wind standard deviation (m/s) for each month of the three reanalyses making up the REM for three zonal regions: 40° - 80° N (top); 10° S - 10° N (middle); and 80° - 40° S (bottom).

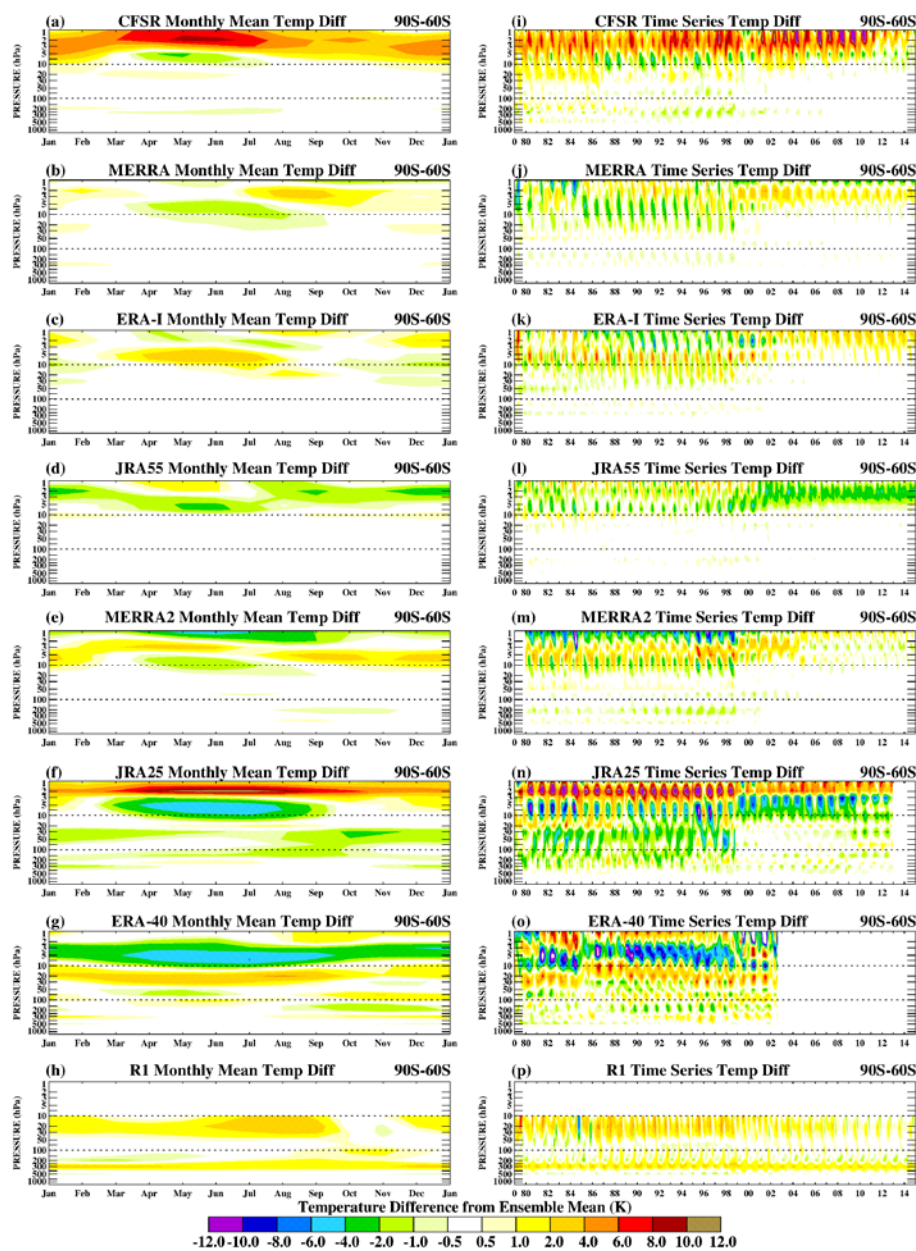


Figure 6. Pressure vs month plots (right) and pressure vs time plots (left) of the temperature difference (K) of individual reanalyses from the REM for the zonal region $90^{\circ} - 60^{\circ}$ S. The reanalyses are a) CFSR, b) MERRA, c) ERA-I, d) JRA-55, e) MERRA-2, f) JRA-25, g) ERA-40, and h) R-1. The left column plots are the monthly mean differences for the entire 1979-2014 period. The right column plots are each month's difference from the REM for that same month.

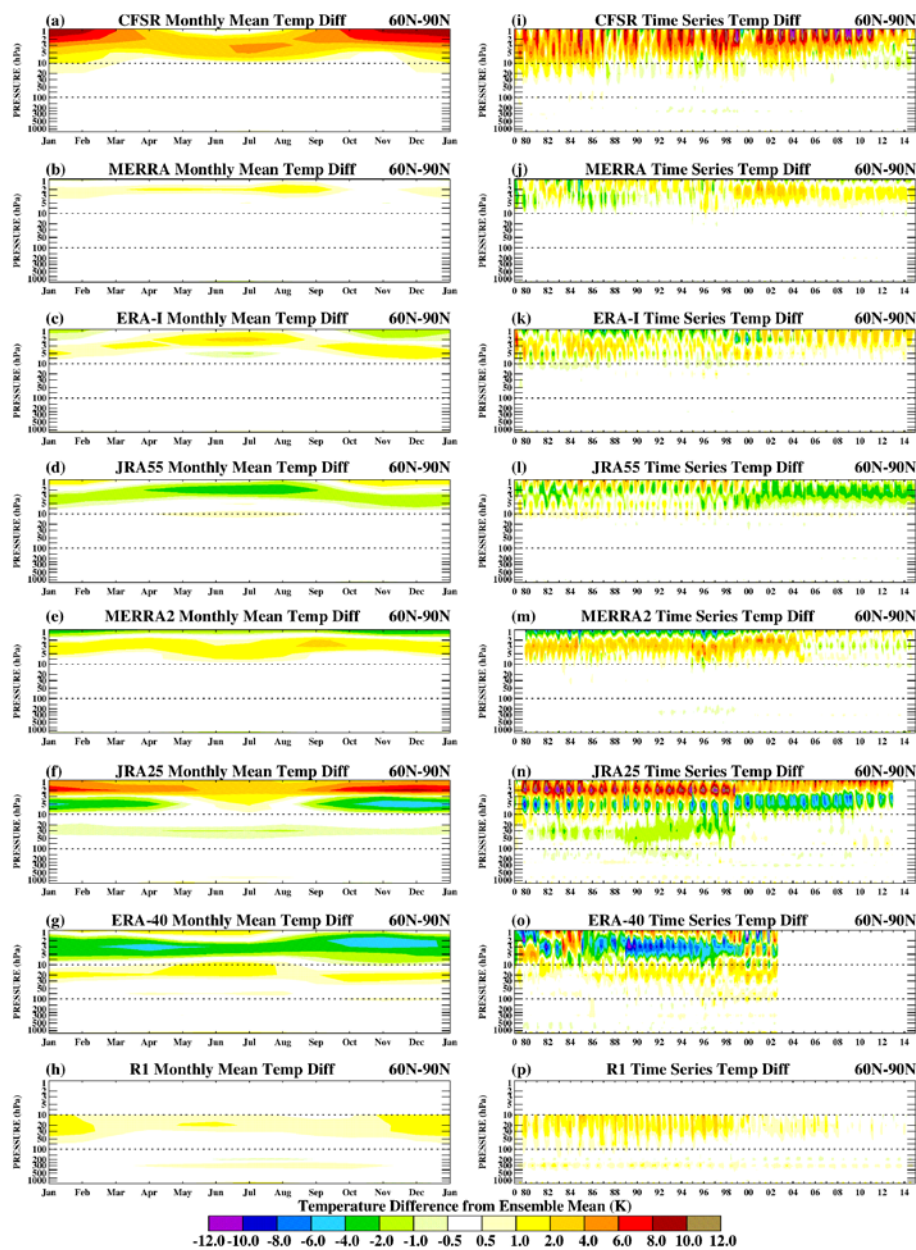


Figure 7. Same as Figure 6 but for the 60° - 90° N latitude zone.

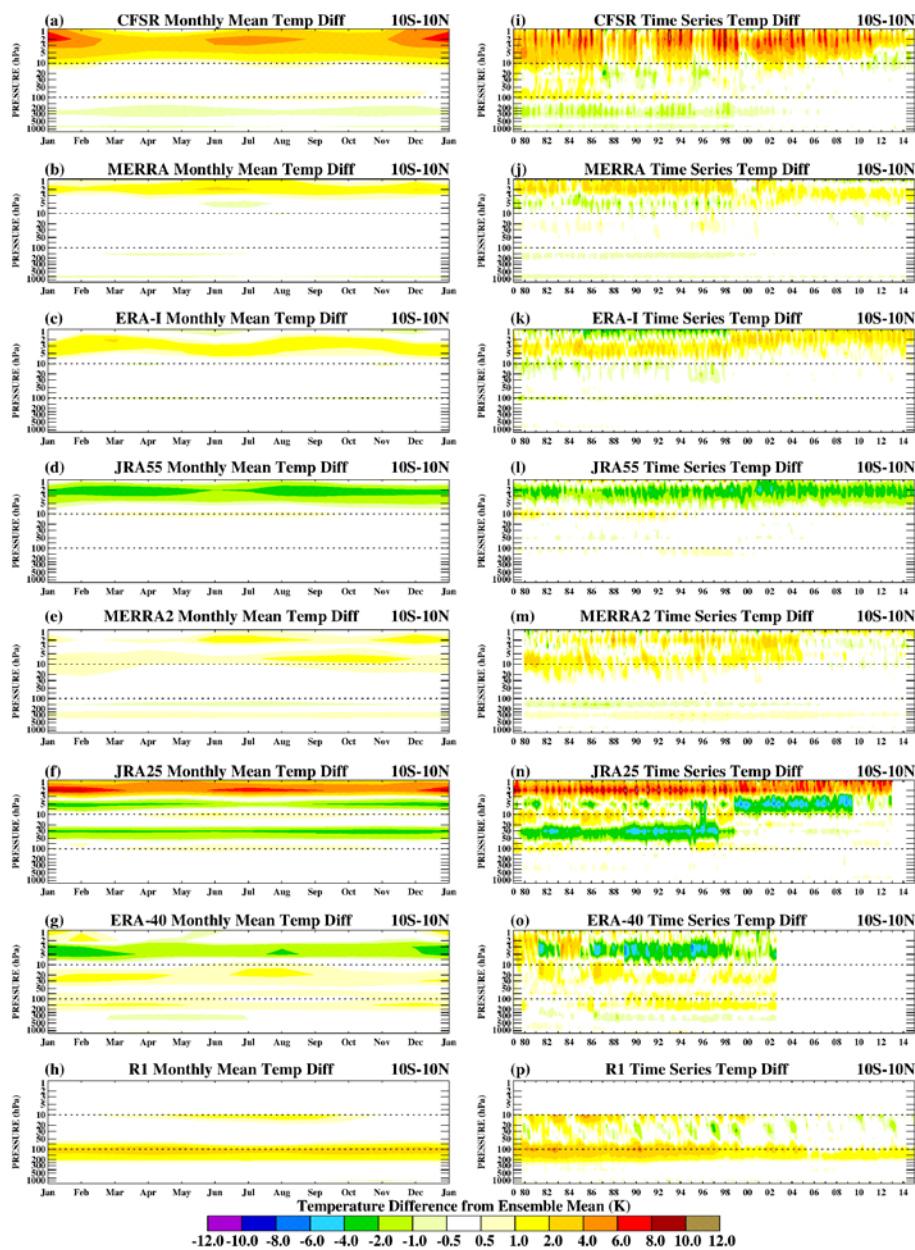


Figure 8. Same as Figure 6 but for the 10° S - 10° N latitude zone.

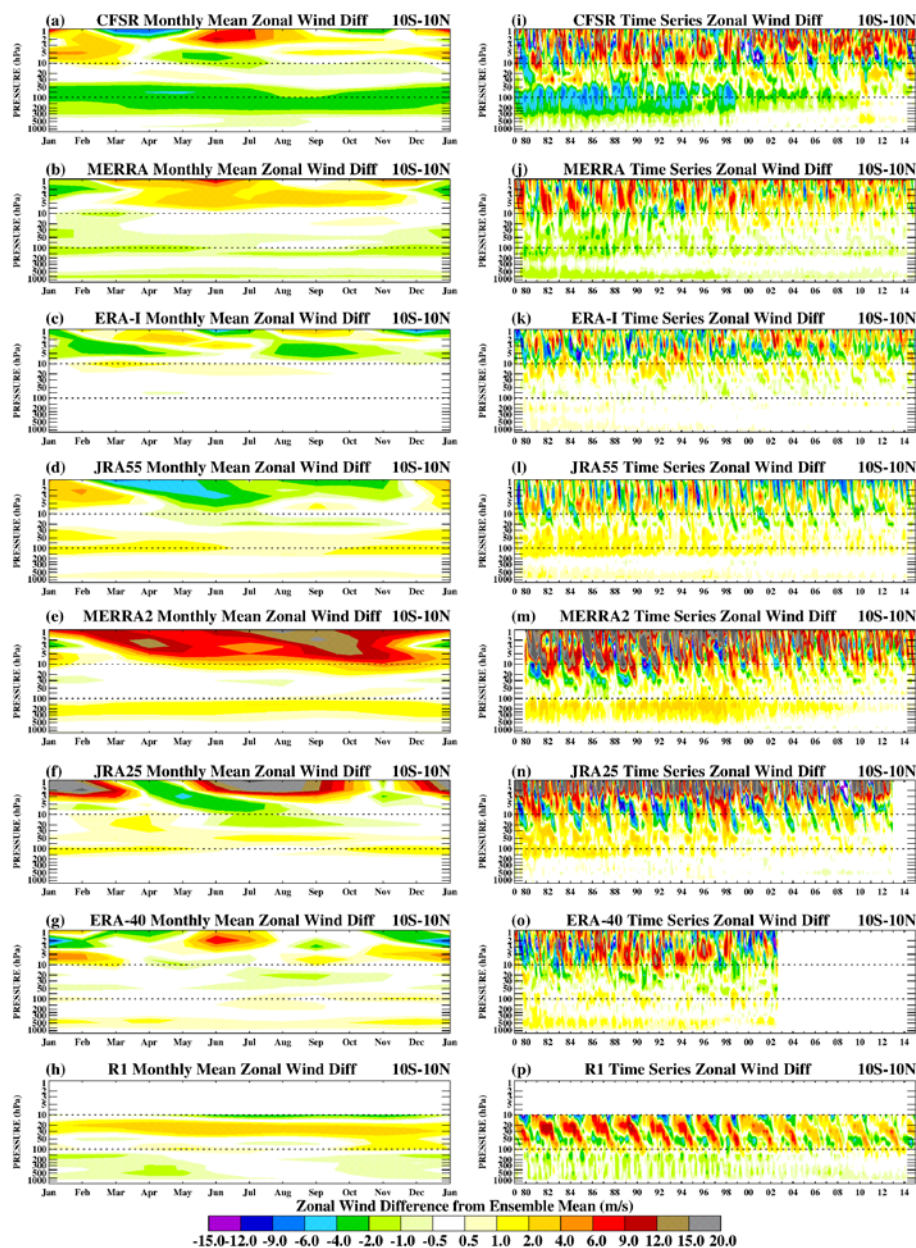


Figure 9. Pressure vs month plots (right) and pressure vs time plots (left) of the zonal wind difference (m/s) of individual reanalyses from the REM for the zonal region 10° S - 10° N. The reanalyses are a) CFSR, b) MERRA, c) ERA-I, d) JRA-55, e) MERRA-2, f) JRA-25, g) ERA-40, and h) R-1.

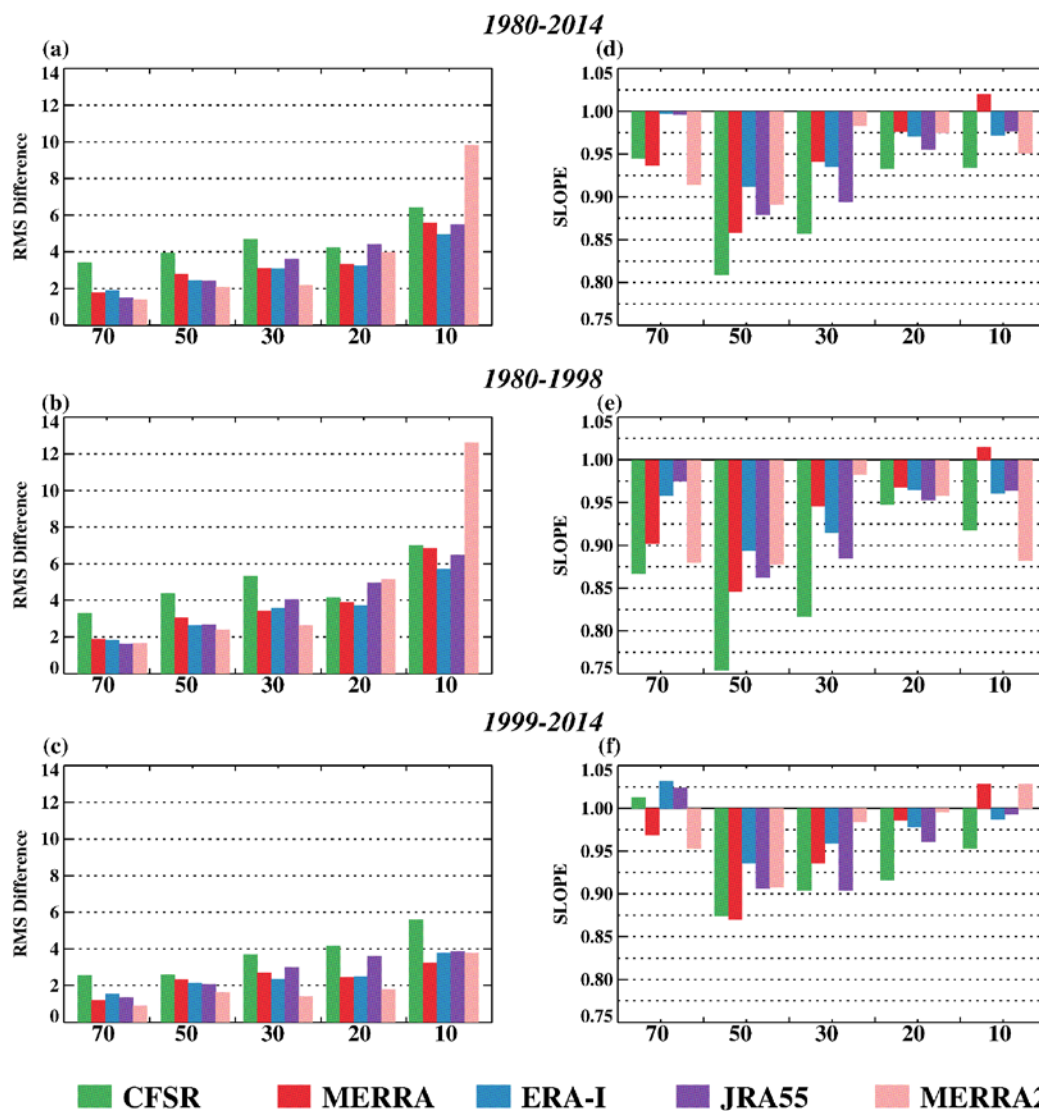


Figure 10. RMS differences (m/s) (left column) and linear slopes (right column) of the matched QBO zonal wind anomalies at 70, 50, 30, 20, and 10 hPa for the CFSR, MERRA, ERA-I, JRA-55 and MERRA-2 reanalyses interpolated to Singapore (1°N, 104°E) versus the observed Singapore monthly mean zonal winds from the FUB. RMS differences and slopes are computed for the 1980-2014 time period (top), the 1980-1998 period (middle), and the 1999-2014 period (bottom). Slopes less than 1.0 indicate that the reanalysis zonal winds are weaker than the Singapore zonal winds.

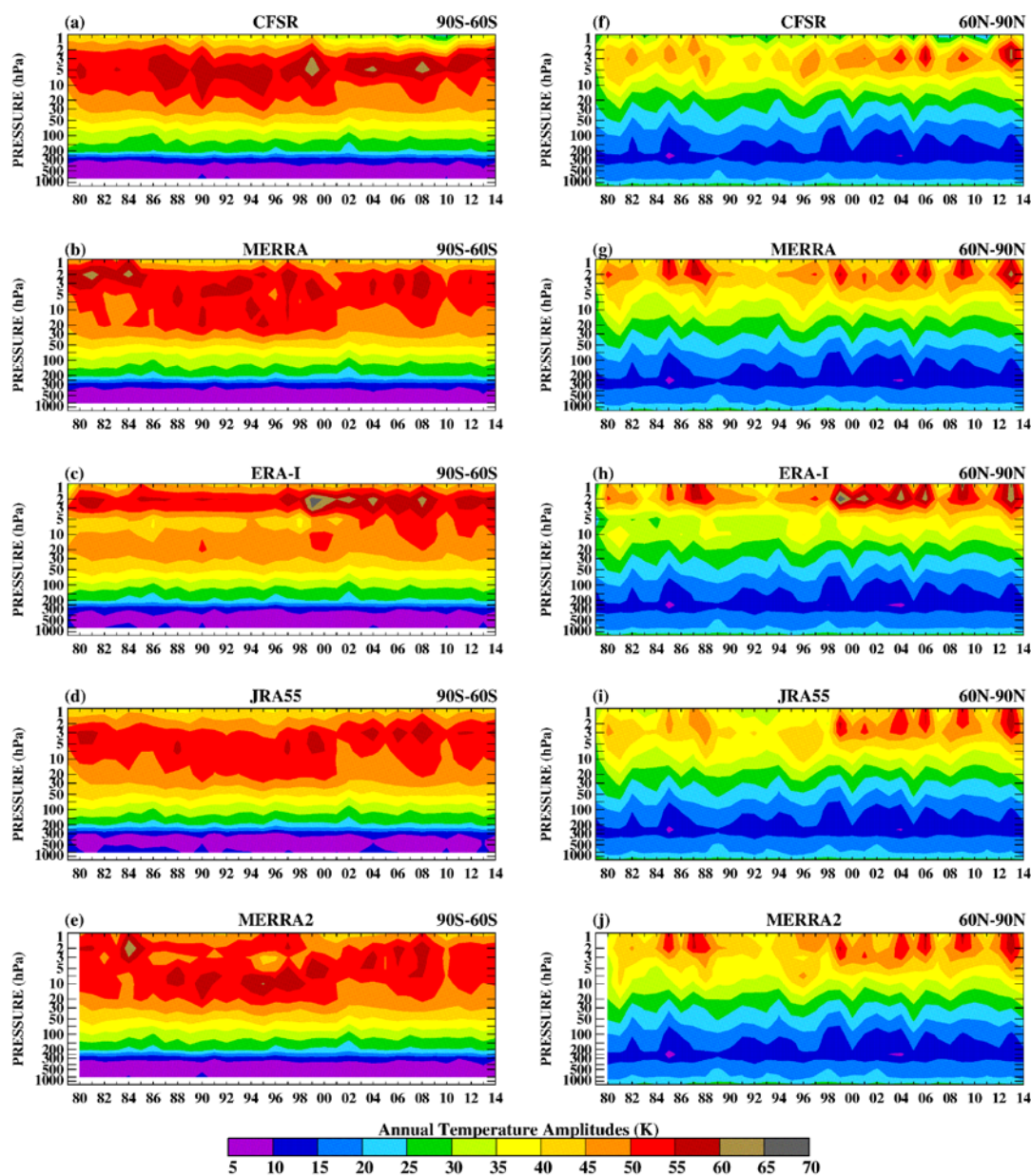


Figure 11. Yearly annual temperature amplitude (K) for $90^{\circ} - 60^{\circ}$ S (left column) and $60^{\circ} - 90^{\circ}$ N (right column) from the a) CFSR, b) MERRA, c) ERA-I, d) JRA55, and e) MERRA-2 reanalyses. Note that the SH annual amplitude is much larger than the NH amplitude. No analysis is performed between 1000 - 700 hPa as this is below the Antarctic surface.

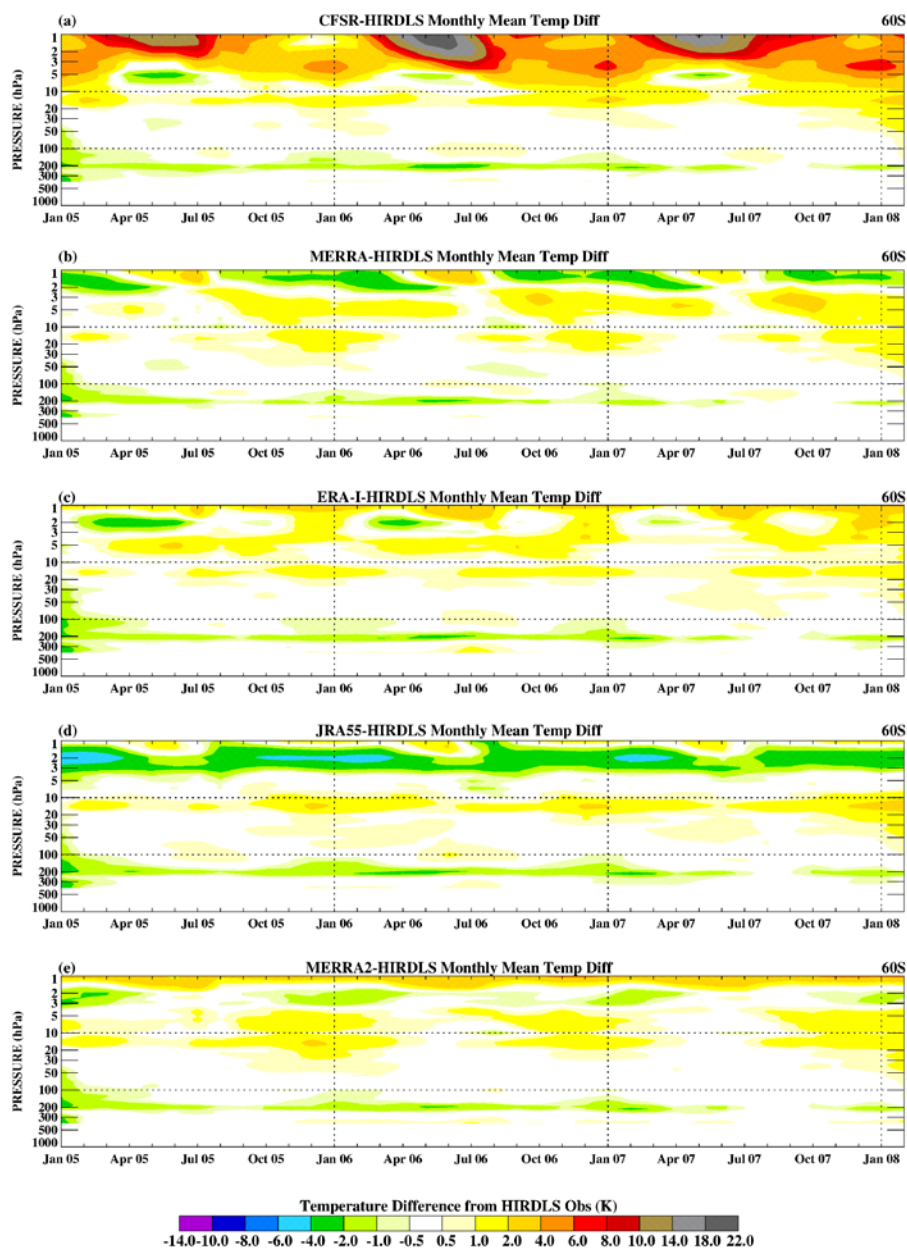


Figure 12. Pressure vs time plot of differences of reanalyses minus HIRDLS temperatures (K) from January 2005 through January 2008 for the Southern Hemisphere high latitude (60° S) zone. The reanalyses are a) CFSR, b) MERRA, c) ERA-I, d) JRA-55, e) MERRA-2.

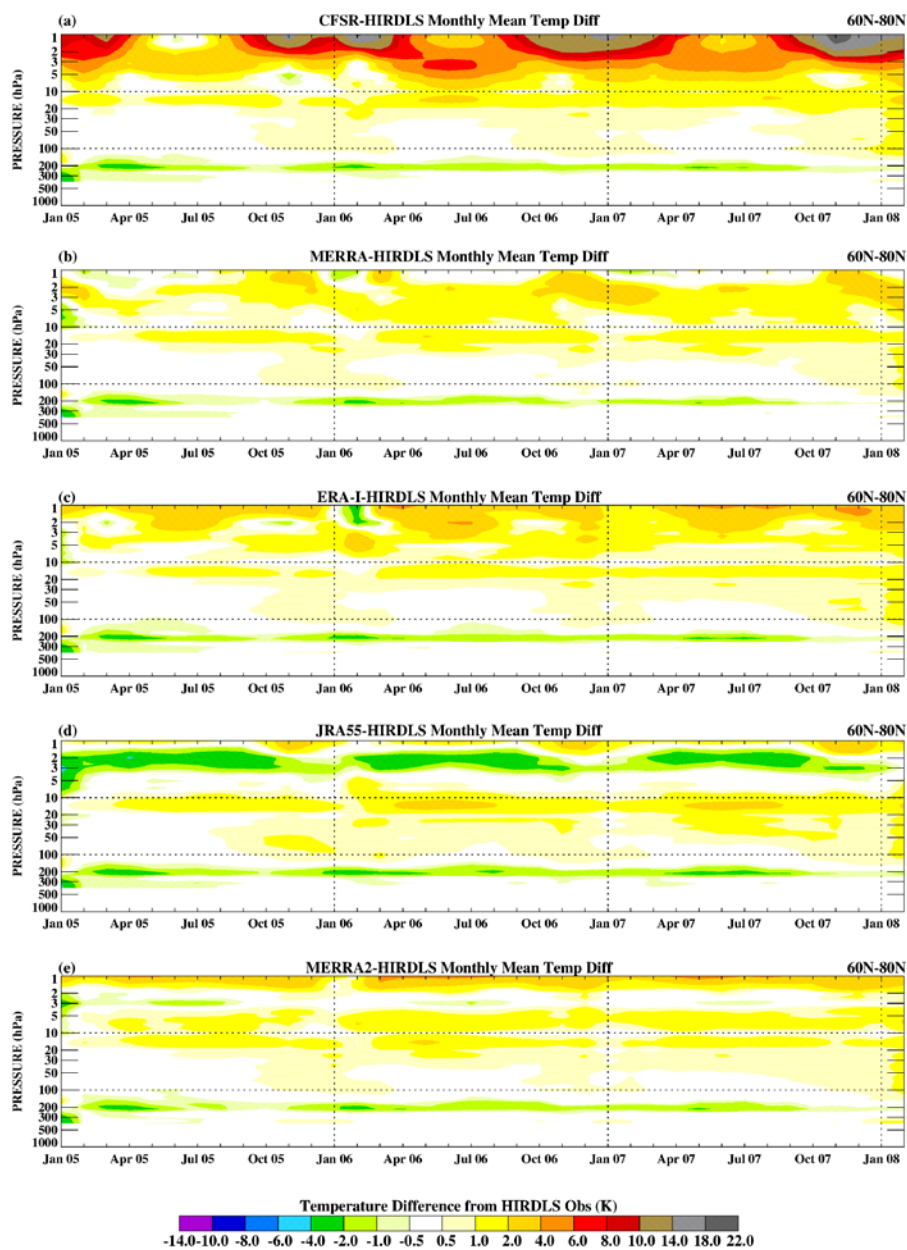


Figure 13. Same as Figure 12 except for the Northern Hemisphere high latitude (60° - 80° N) zone.

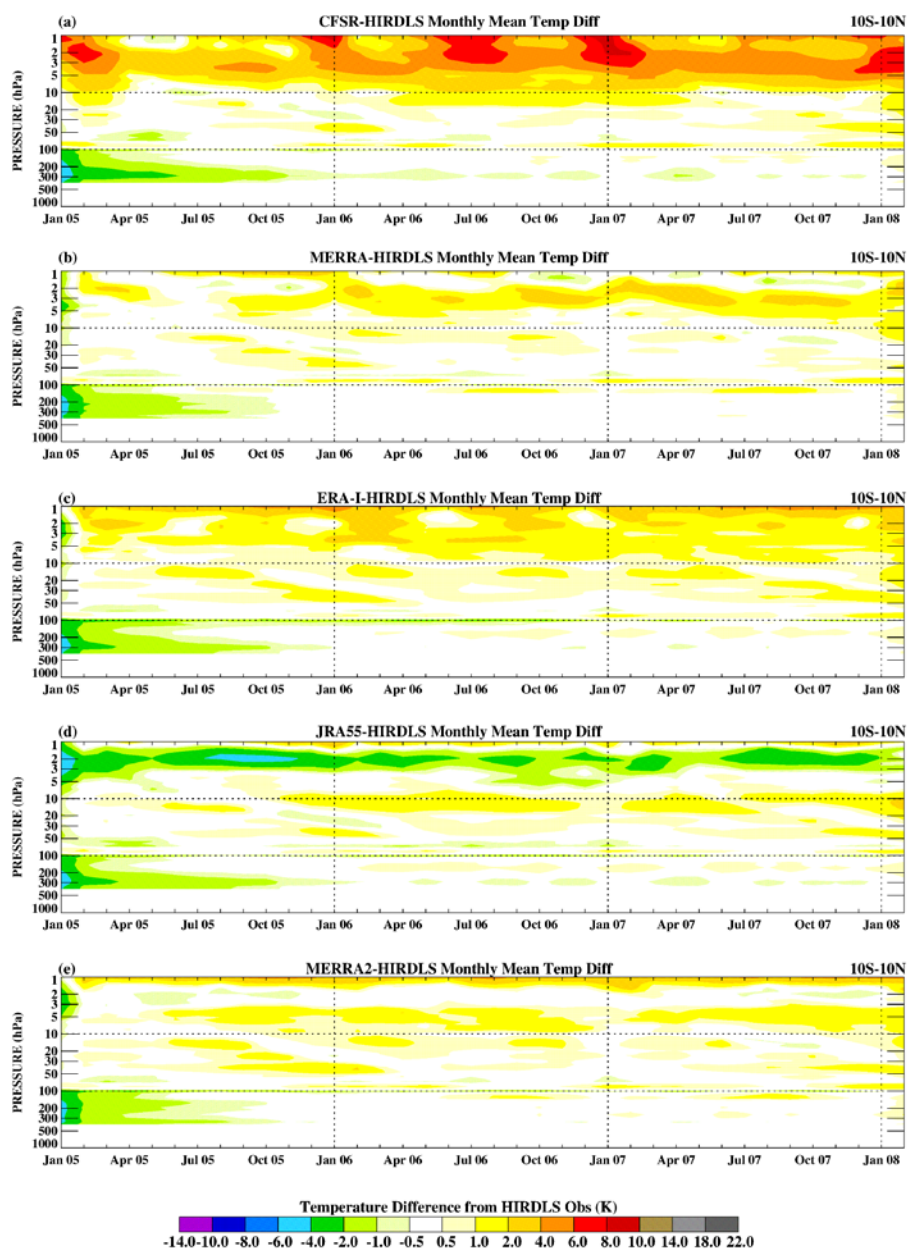


Figure 14. Same as Figure 12 except for the Equatorial latitude (10° S – 10° N) zone.

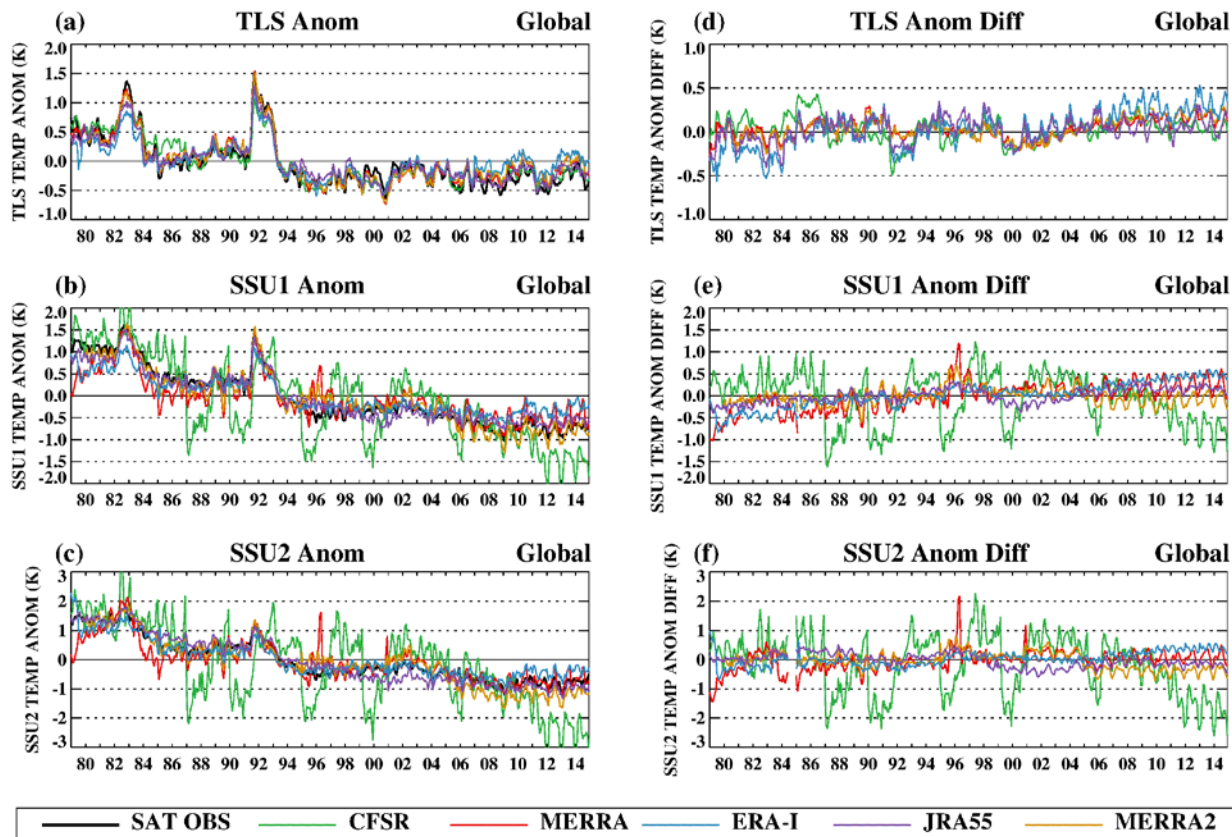


Figure 15. Time series plots of layer mean temperature anomalies (K) from the 1980-2010 climatology for the lower stratosphere (TLS) equivalent to the MSU 4 observations (top), the middle stratosphere (SSU1) equivalent to the SSU channel 1 observations (middle), and the upper stratosphere (SSU2) equivalent to the SSU channel 2 observations (bottom). TLS, SSU1 and SSU2 weights are applied to the CFSR, MERRA, ERA-I, JRA-55, and MERRA-2 pressure level data to produce layer mean temperatures and anomalies. NOAA/STAR TLS, SSU1, and SSU2 anomalies are plotted along with the reanalyses in the left column. Reanalyses anomaly differences from the NOAA/STAT anomalies are plotted in the right column.